frontiers | Frontiers in Marine Science

TYPE Original Research
PUBLISHED 13 October 2022
DOI 10.3389/fmars.2022.944141

OPEN ACCESS

EDITED BY
Nina Yasuda,
The University of Tokyo, Japan

REVIEWED BY
David Bourne,
James Cook University, Australia
Andrew WB Johnston,
University of East Anglia,
United Kingdom
Shinya Shikina,
National Taiwan Ocean University,
Taiwan

*CORRESPONDENCE
Rafel Simó
rsimo@icm.csic.es

†PRESENT ADDRESS
Stephanie G. Gardner,
Centre for Marine Science and Innovation, University of New South Wales Sydney, NSW, Australia

SPECIALTY SECTION
This article was submitted to Coral Reef Research, a section of the journal Frontiers in Marine Science

RECEIVED 14 May 2022
ACCEPTED 30 August 2022
PUBLISHED 13 October 2022

CITATION
Masdeu-Navarro M, Mangot J-F, Xue L, Cabrera-Brufau M, Gardner SG, Kieber DJ, González JM and Simó R (2022) Spatial and diel patterns of volatile organic compounds, DMSP-derived compounds, and planktonic microorganisms around a tropical scleractinian coral colony. *Front. Mar. Sci.* 9:944141. doi: 10.3389/fmars.2022.944141

Spatial and diel patterns of volatile organic compounds, DMSP-derived compounds, and planktonic microorganisms around a tropical scleractinian coral colony

Marta Masdeu-Navarro[1], Jean-François Mangot[1], Lei Xue[2], Miguel Cabrera-Brufau[1], Stephanie G. Gardner[1†], David J. Kieber[2], José M. González[3] and Rafel Simó[1*]

[1]Department of Marine Biology and Oceanography, Institut de Ciències del Mar (ICM-CSIC), Barcelona, Spain, [2]Department of Chemistry, State University of New York, College of Environmental Science and Forestry, Syracuse, NY, United States, [3]Department of Microbiology, University of La Laguna, La Laguna, Spain

Volatile organic compounds (VOCs) are constituents of marine ecosystems including coral reefs, where they are sources of atmospheric reactivity, indicators of ecosystem state, components of defense strategies, and infochemicals. Most VOCs result from sunlight-related processes; however, their light-driven dynamics are still poorly understood. We studied the spatial variability of a suite of VOCs, including dimethylsulfide (DMS), and the other dimethylsulfoniopropionate-derived compounds (DMSPCs), namely, DMSP, acrylate, and dimethylsulfoxide (DMSO), in waters around colonies of two scleractinian corals (*Acropora pulchra* and *Pocillopora* sp.) and the brown seaweed *Turbinaria ornata* in Mo'orean reefs, French Polynesia. Concentration gradients indicated that the corals were sources of DMSPCs, but less or null sources of VOCs other than DMS, while the seaweed was a source of DMSPCs, carbonyl sulfide (COS), and poly-halomethanes. A focused study was conducted around an *A. pulchra* colony where VOC and DMSPC concentrations and free-living microorganism abundances were monitored every 6 h over 30 h. DMSPC concentrations near the polyps paralleled sunlight intensity, with large diurnal increases and nocturnal decrease. rDNA metabarcoding and metagenomics allowed the determination of microbial diversity and the relative abundance of target functional genes. Seawater near coral polyps was enriched in DMS as the only VOC, plus DMSP, acrylate, and DMSO, with a large increase during the day, coinciding with high abundances of symbiodiniacean sequences. Only 10 cm below, near the coral skeleton colonized by a turf alga, DMSPC concentrations were much lower and the microbial community was significantly different. Two meters down current from the coral, DMSPCs decreased further and the microbial community was more similar to that near the polyps than that near the turf alga. Several DMSP cycling genes were enriched in near-polyp with respect to down-current waters, namely, the eukaryotic DMS production and

DMS oxidation encoding genes, attributed to the coral and the algal symbiont, and the prokaryotic DMS production gene *dddD*, harbored by coral-associated *Gammaproteobacteria*. Our results suggest that solar radiation-induced oxidative stress caused the release of DMSPCs by the coral holobiont, either directly or through symbiont expulsion. Strong chemical and biological gradients occurred in the water between the coral branches, which we attribute to layered hydrodynamics.

KEYWORDS

VOC, DMS, DMSP, acrylate, DMSO, coral, *Symbianodiciaea*, seaweed

Introduction

Coral reefs are highly diverse and productive ecosystems that thrive in oligotrophic waters of tropical and subtropical oceans (Hoegh-Guldberg et al., 2017). Reefs are built by calcifying scleractinian coral colonies that provide diverse and interdependent habitats to all kinds of organisms, including vertebrate and invertebrate animals, seaweeds, and microbes. The coral colony itself is a multi-organism consortium of the cnidarian, the symbiont microalgae, and a myriad of microorganisms associated with the coral tissues and exudates, with the whole entity being named the coral holobiont (Rohwer et al., 2002).

Coral reefs provide key ecosystem services: biodiversity, coastal protection, biogeochemical cycling, fisheries, provision of raw materials, and cultural benefits (Woodhead et al., 2019). Recently, an ecosystem service of short-term regulation of regional climate has been suggested too, at least for the large extending Great Barrier Reef (Jones, 2015; Jackson et al., 2020). This climate effect would operate from the observed capacity of coral reefs to emit volatile sulfur in the form of dimethylsulfide (DMS). In the atmosphere, emitted DMS oxidizes to form precursors of aerosols that enhance the formation, lifetime, and brightness of low-level clouds (Charlson et al., 1987; Simó, 2001), and thereby potentially reduce incident solar irradiance and temperature. Since the production and emission of DMS from coral reefs is triggered under higher irradiance and temperature, this reef–atmosphere interaction could potentially act as a regional thermostat (Jackson et al., 2020). This hypothesis is currently under scrutiny.

Sulfur emission for cloud seeding is not the only way coral reefs affect the overlying atmosphere. Tropical reefs are also suggested to be hot spots for the emission of biogenic volatile organic compounds (VOCs) beyond DMS (Exton et al., 2015). VOCs are sources of atmospheric reactivity, indicators of the ecosystem state, defense strategies, and chemical cues for organism–organism communication, e.g., to facilitate foraging. Ongoing studies are paving the road towards characterizing the volatilome at the reef ecosystem level, and they have revealed a diverse VOC composition (Lawson et al., 2020; 2021). While VOCs are being discovered that were unknown to marine systems, a look at the VOC whose production processes and ecological impacts are known will be informative of the physiological, ecosystem, and environmental functions they sustain.

Carbonyl sulfide (COS) is the most abundant and most stable sulfur gas in the atmosphere (Lennartz et al., 2020). Emitted by the biosphere and the oceans through the interaction of solar radiation and dissolved organic matter, it reaches the stratosphere where it influences ozone destruction and aerosol formation. Carbon disulfide (CS_2) is another sulfur volatile produced in the surface ocean by photochemistry and phytoplankton, and in sediments by microbial activity (Kim and Andreae, 1992). It further contributes to the atmospheric COS burden through oxidation (Lennartz et al., 2020). Whether coral reefs are significant producers of COS and CS_2 is unknown. Isoprene (C_5H_8) is another VOC that is best known for being the most abundantly produced by the global biosphere, one that affects the oxidative capacity of the troposphere owing to its reactivity with airborne oxidants. It is released by vascular plants and trees as a response to alleviate thermal stress; in the ocean, it is produced mainly by phytoplankton, but the mechanisms remain unclear (McGenity et al., 2018). Tropical coral holobionts also produce isoprene, but there is no consensus as to whether it arises from physiological stress (Swan et al., 2016; Dawson et al., 2021; Lawson et al., 2021). Halomethanes (halogenated C1 compounds) are commonly found in coastal ecosystems, where they are produced mainly by seaweeds, and to a lesser extent by phytoplankton, to combat oxidative stress (Carpenter et al., 2012). They have also been suggested to be involved in defense mechanisms. In the atmosphere,

halomethanes affect oxidant radicals and participate in tropospheric and stratospheric ozone destruction (Saiz-López and von Glasow, 2012). Whether coral holobionts are relevant sources of halomethanes is unknown.

Corals are known to undergo fundamental physiological changes in response to incident light during a diel cycle. They switch from autotrophic holobiont during the day, when the algal symbionts fix carbon and produce oxygen, to heterotrophs at night, when polyps prey on plankton and the animal respiration is higher due to digestion (Schneider et al., 2009). This physiological switch results in hyperoxic conditions in the holobiont during the day, and hypoxia at night. Among the suite of physiological responses to diurnal oxidative stress (Hemond and Vollmer, 2015), many hermatypic coral holobionts use dimethylsulfoniopropionate-derived compounds (DMSPCs) as antioxidants (e.g., Deschaseaux et al., 2014b). DMSP is an osmolyte in many algal taxa, including the coral symbionts *Symbiodiniaceae*. DMSP is such an abundant compound in the marine environment that it carries a large share of carbon and sulfur trophic transference in marine microbial food webs, and is a potent infochemical in foraging interactions, an antioxidant, and the source of climate-active DMS (Simó, 2001; Carpenter et al., 2012). In tropical coral holobionts, DMSP is synthesized not only by the algal symbionts (Deschaseaux et al., 2014a) but also by the cnidarian (Raina et al., 2013) and associated bacteria (Kuek et al., 2022). DMSP can be enzymatically cleaved to DMS and acrylate, a catabolic route that is thought to be the most instrumental for alleviating oxidative stress (Sunda et al., 2002), or it can be catabolized through demethylation and demethiolation, a route that leads to sulfur incorporation by the consumer (Howard et al., 2006).

We conducted a study in the shallow reefs of Mo'orea, in the French Polynesia, to describe the distributions of VOCs and DMSPCs around dominant reef-forming organisms and learn about their sources and drivers. To this aim, we studied the spatial variability of a suite of VOCs and DMSPCs in waters around colonies of two scleractinian corals (*Acropora pulchra* and *Pocillopora* sp.) and the brown seaweed *Turbinaria ornata*. We also conducted a dedicated study around an *A. pulchra* colony over a diel cycle. Taxonomic (rDNA metabarcoding) and functional (metagenomics) gene analyses helped to propose the most likely candidate organisms responsible for the diel DMSPC pattern observed. A companion paper reports the turnover of dissolved DMSP and acrylate in our study site (Xue et al., 2022).

Materials and methods

Study area

Fieldwork was conducted between 4 and 27 April 2018, on the north and northeast coast of the island of Mo'orea, French Polynesia (Figure 1A). On the inner side, the reef crest harbors large patches of *Acropora* spp. colonies and smaller patches of *Pocillopora* spp. and other corals, and there is an abundant population of the brown algal seaweed *T. ornata*. On the outer side, the forereef platform is mainly composed of the cauliflower coral *Pocillopora* spp.

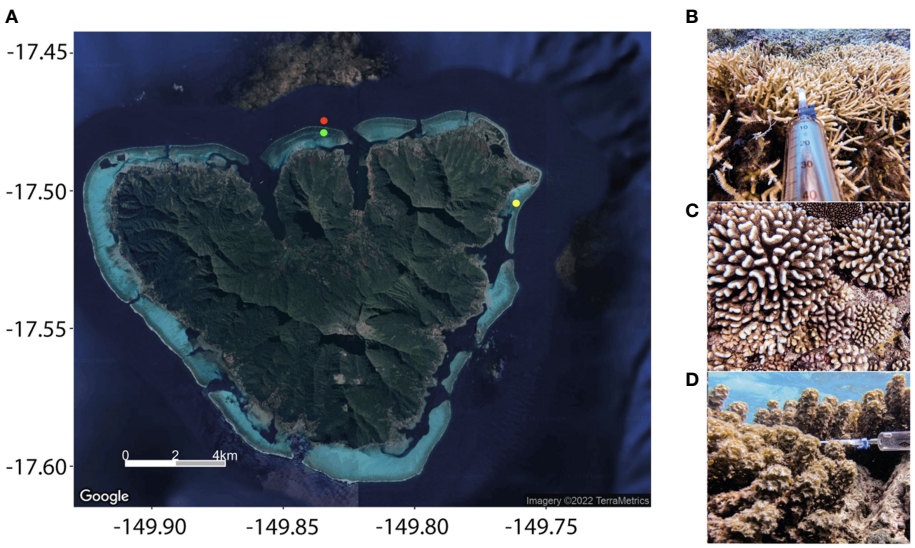

FIGURE 1
(A) Location of the sampling sites in Mo'orea. Zoom into the fore reef and back reef sampling sites in the northern coast, off Cook's Bay, and into the back reef sampling site in the Tema'e Beach reef, along the northwestern coast, where the diel study was conducted. Images of **(B)** *Acropora pulchra*, **(C)** *Pocillopora* sp., and **(D)** *Turbinaria ornata*, with the all-glass syringe used to collect seawater.

Sample collection and storage

Gradients around colonies. Water samples (0.5 L) for DMSPC and VOC measurements were taken from the interstitial space of, and nearby, two coral colonies and a seaweed patch (Figures 1B–D). One pair of seawater samples around the coral *Acropora pulchra* [AP(A)] was collected on 18 April; a second pair [AP(B)] was collected on 23 April, both at 1-m depth within the Tema'e Beach reef (17.501°S, 149.759°E), northeast coast (Figure 1A). The *A. pulchra* thicket had a diameter of several meters. In the same reef, another pair of seawater samples was collected around a 0.5-m-sized colony of the coral *Pocillopora* sp. [P(A)], at a depth of 2 m. Another pair of samples around a similar *Pocillopora* sp. colony [P(B)] was taken on 17 April at the forereef of the northern coast (17.475°S, 149.839°E), at a depth of about 3 m. Seawater samples around the brown seaweed *T. ornata* (TO) were collected on 16 April in the back reef of the northern coast (17.478°S, 149.839°E), approximately at 1 m depth. The seaweed thicket was 0.5–1 m large. In all cases, the pair of samples corresponded to a first sampling point as close as possible (~0.5 cm) to the organism without touching it, between the branches of *A. pulchra*, the verrucae of *Pocillopora* sp., or the thalli of *T. ornata* (IN), and a second sampling point 2 m away from the target organism (OUT).

Diel cycle. A diel study was conducted around an *A. pulchra* colony in the Tema'e Beach reef. Water samples were withdrawn from three different sampling points around the colony, at a depth of ~1 m (Figure 2): (IN) between the living branches, ~1 cm next to the polyps; (AL) deeper between the branches, ~0.5 cm next to the coral skeleton colonized by turf algae; and (OUT) 2 m down current from the patch over a sandy bottom ~2 m deep. Over 36 consecutive hours between 24 and 25 April, sampling was done at 07:00, 12:00, 17:00, 00:00, 07:00, and 12:00 local time. An adjacent coral colony was marked with flagging tape to facilitate location of the sampling site, so that samples were taken from the same branches at each time point. In the first five time points, 0.5 L of seawater was collected for the DMSP-derived compounds, VOC, and microbial abundance measurements. For the last time point only (12:00 on 25 April), 0.8 L was taken from IN and AL, and 2.5 L from OUT, to have enough volume for microbial DNA analysis.

Sampling protocol. All samples were collected using glass bottles that were rinsed three times with *in situ* seawater before sampling. For the IN and AL samples, water was withdrawn through 0.318-cm OD PTFE tubing attached to a 50-ml all-glass syringe *via* a three-way polycarbonate valve (Figure 1B), and transferred into the glass bottle avoiding bubble generation. The process was repeated until the bottle was full without headspace, so that approximately 10 individual samples were aggregated in a bottle. For the OUT samples, the bottle was filled directly without the syringe. Only one bottle was collected from IN, AL or OUT. Once all the bottles were filled and sealed with solid, ground-glass stoppers, the bottles were transported to the shore and driven to the lab for analysis within 1–2 h after collection.

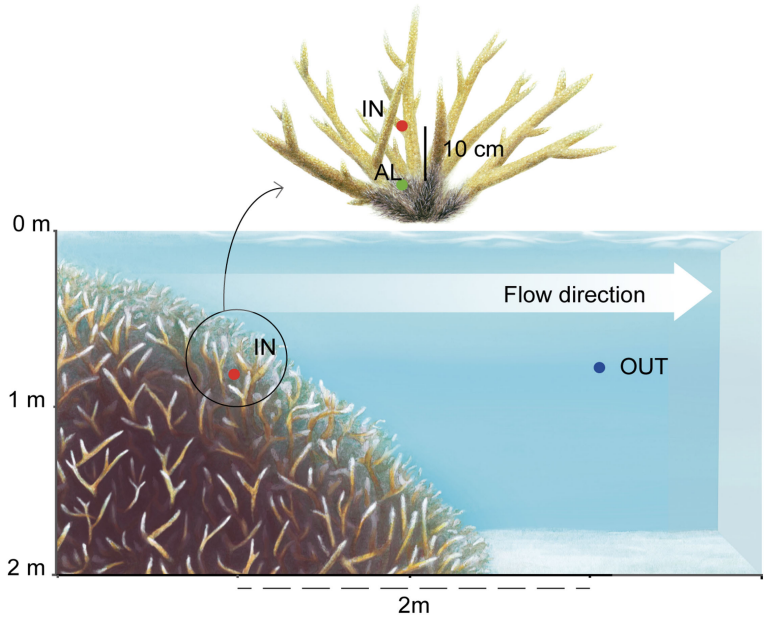

FIGURE 2
Scheme of sampling points in the diel study of *Acropora pulchra* in the Tema'e Beach reef. IN: between the living branches; AL: 10 cm deeper, next to the dead skeleton colonized by turf algae; OUT: 2 m down current from the patch. Artwork by J. Mir-Arguimbau.

Microbial abundances

For enumeration of heterotrophic prokaryotes (including bacteria and archaea) and pico- and nano-phytoplankton, 2- to 5-ml sample aliquots were fixed with glutaraldehyde (0.5%) and stored at −80°C until analysis based on size and fluorescence on a flow cytometer (CyFlow Cube 8, Sysmex Partec). Heterotrophic prokaryotes (including bacteria and archaea) were stained with SYBRgreen I (∼20 µM final concentration) prior to quantification by green fluorescence. Prokaryotic and eukaryotic pico- and nano-phytoplankton were counted based on their red and orange autofluorescence.

VOC concentrations

For VOC analyses, we used an Agilent 5975T LTM gas chromatograph–mass spectrometer coupled to a Stratum (Teledyne Tekmar) purge and trap system. Seawater aliquots (25 ml) were taken from the sample bottles with an Artiglass syringe with a PTFE tube. After removal of air bubbles, the PTFE tube was replaced with a GF/F filter holder that was attached to the inlet of the sparge vessel *via* a Luer lock fitting, and the aliquot was filter injected. VOC were sparged at room temperature for 12 min with a flow rate of 40 ml/min of ultrapure He, trapped on a VOCARB 3000 absorption column held at room temperature, and desorbed by heating to 250°C. VOCs were separated in a capillary column LTM DB-VRX (Agilent; 20 m × 0.18 mm × 1 µm) held at 35°C for 4 min, then heated to 230°C at 30°C/min, and held at 230°C for 4 min, making a total analysis time of 14.5 min. The He carrier gas flow rate was 0.8 ml/min. Compounds were detected by an electron impact ionization mass spectrometer in selected ion monitoring mode. Target compounds [COS, C_2H_6S (DMS), CS_2, $C_2H_6S_2$ (DMDS), CH_3I, CH_2ClI, CH_2Br_2, and $CHBr_3$] were identified matching the retention times of their most characteristic (quantification) ions and their confirmation ions with those of pure standards (Table S1). Each sample was analyzed in duplicate.

DMSP, DMSO, and acrylate concentrations

For total DMSP (DMSPt, i.e., dissolved + particulate) analysis, we stored 40 ml of unfiltered seawater in crimped glass vials after adding two NaOH pellets (45 mg each, ∼0.2 mol L^{-1} final concentration, pH >12). The DMSPt + DMS was determined as evolved DMS after undergoing alkaline hydrolysis for 1–2 months. Evolved DMS was analyzed back in the lab with a purge-and-trap system coupled to a gas chromatograph (Shimadzu GC14A) with flame photometric detection. The DMSPt concentration was calculated by subtraction of the on-site determined DMS concentration. All analyses were run in duplicate, and standard errors for both DMS and DMSP concentrations fell within 10% of the mean.

To determine dissolved DMSP (DMSPd), acrylate and DMSO concentrations, 15-ml sample aliquots were gravity filtered using precombusted, 25-mm-diameter GF/F filters into 20-ml scintillation vials using the small-volume drip filtration method described by Kiene and Slezak (2006). Filtered samples were microwaved to boiling, bubbled with high-purity nitrogen gas to remove DMS, and acidified with 150 µl of Ultrex HCl (Kinsey and Kieber, 2016). All samples were stored at room temperature in the dark until analysis in the lab. For DMSPd analysis, 200 µl of 5 M NaOH was added to 1 ml of seawater samples in precleaned, gas-tight borosilicate serum vials, which were reacted overnight at room temperature in the dark. Evolved DMS was analyzed using a cryogenic purge-and-trap system and a Shimadzu GC-14A gas chromatograph with a flame photometric detector (Kinsey et al., 2016). Acrylate concentrations were determined using a pre-column derivatization HPLC method that provided sufficient sensitivity for the analysis of sub-nanomolar acrylate concentrations in seawater (Tyssebotn et al., 2017). For derivatization, 300 µl of 20 mM TSA reagent in MeOH was pipetted into a 5-ml precleaned borosilicate vial containing 3 ml of a standard or seawater sample. Following pH adjustment to 4.0, each vial was tightly screw-capped and incubated in a 90°C water bath for 6 h. After cooling to room temperature, each derivatized sample was first filtered using a 0.2-µm Nylon syringe filter (Pall) followed by a 1-ml injection of each filtered sample on a reverse-phase Water HPLC column with UV detection at 257 nm to quantify the acrylate-TSA derivative. The limit of detection of this method was 0.2 nM for a 1-ml injection with a signal-to-noise ratio of 2.

For total and dissolved DMSO analysis, 1 ml of the same unfiltered or filtered seawater samples used for DMSP analysis were added 200 µl of 20% TiCl3 in precleaned borosilicate serum vials, which were incubated at 55°C in a water bath for 1 h. Evolved DMS was measured as above.

Solar radiation

The diel cycle of sunlight was provided by the meteorological station at the Gump Research Station (Washburn and Brooks, 2022), located 6 km away from our sampling site at Tema'e Beach. Meteorological data include air temperature, relative humidity, wind speed and direction, global solar radiation, atmospheric pressure, and integrated rainfall. Data are available every 5 min from August 2006 to the present day. Postprocessing of these data consisted of unit conversion and exclusion of corrupted data records.

DNA extraction, 16S/18S rRNA gene amplicon, and metagenomic sequencing

Samples for DNA collection from waters around the *A. pulchra* colony were taken from the remaining volumes [ca. 0.8 L (IN, AL) and 2.45 L (OUT)] of the samples collected at noon on the second day of the diel cycle. Samples were prefiltered through a 200-µm mesh, and the microbial biomass was collected on 0.2-µm pore-size, 47-mm-diameter polycarbonate filters using a peristaltic pump. The filters were flash frozen in liquid N_2 and stored at −80°C. Total DNA was extracted using the phenol-chloroform protocol as described in Massana et al. (1997). Prokaryotic and eukaryotic diversities were determined by amplicon sequencing of the V4/V5 and V4 regions of the 16S and 18S rDNA genes, respectively, using the Illumina MiSeq platform and paired-end reads (2 × 250 bp). PCR amplifications were done using (1) the prokaryotic universal primers 515F-Y (5'-GTGYCAGCMGCCGCGGTAA-3') and 926R (5'-CCGYCAATTYMTTTRAGTTT-3') (Parada et al., 2016), and (2) the eukaryotic universal primers V4F (5'-CCA GCA SCY GCG GTAATT CC-3') and V4R (5'-ACTTTC GTT CTT GAT YRR-3') (Balzano et al., 2015). All samples were sequenced at the Research and Testing Laboratories (RTL, Lubbock, TX, USA).

The presence and abundance of genes involved in the DMS/DMSP cycling were determined by metagenomics. Whole metagenome sequencing of DNA extracts from IN and OUT samples (attempt to sequence AL failed) was performed using a PCR-free protocol at the Centre Nacional d'Anàlisi Genòmica (CNAG, Barcelona, Spain; http://cnag.cat/). Short-insert paired-end libraries were prepared with the Illumina TruSeq Sample Preparation kit (Illumina Inc.) and sequenced on a NovaSeq 6000 Illumina platform (2 × 150 bp), yielding about 45 Gb of sequencing information per metagenome.

Amplicon data processing

Primers and spurious sequences from the amplicon sequencing data obtained from both prokaryotic and eukaryotic communities (16S and 18S rDNA sets, respectively) were trimmed from the forward and reverse reads using cutadapt v2.3 (Martin, 2011) with the default error tolerance and a minimum overlap equal to half the primer length. Trimmed reads were subsequently processed with DADA2 v1.4 (Callahan et al., 2016). On the basis of quality profiles, forward reads of the 16S and 18S rDNA sets were respectively truncated at 245 and 250 bp, respectively, and reverse reads were respectively truncated at 180 and 220 bp; reads with more than two expected errors [maxEE = c(2,2)], a quality score lower than two (truncQ = 2), and ambiguous nucleotides (Ns) were excluded.

Forward and reverse reads were then independently corrected using run-specific error-rate modeling and dereplicated. Corrected paired-end reads were subsequently merged to produce amplicon sequence variants (ASVs). Chimeric ASVs were identified and discarded from both datasets. Next, ASVs were taxonomically assigned using the Ribosomal Database Project naïve Bayesian classifier (Wang et al., 2007), as implemented in DADA2, and an 80% minimum bootstrap confidence threshold using SILVA (v132; Pruesse et al., 2007) and PR^2 (v4.11.1; Guillou et al., 2012) as reference databases for the 16S and 18S rDNA sets, respectively. For the 16S rDNA set, singletons and sequences affiliated to eukaryotes, organelles, or chloroplasts were removed prior to subsequent analyses. Singletons were also removed to build the 18S rDNA dataset. Since special attention was paid to the unicellular eukaryotic community members (i.e., protists), the sequences affiliated to metazoans, *Embryophyceae* (land plants), *Rhodophyta* (red algae), *Ulveophyceae* (*Chlorophyta*, green algae), and *Phaeophyceae* (brown algae) were removed, because their large 18S rRNA gene copy numbers and multicellularity would bias the data against the contribution of protistan taxa. To enable comparisons between samples, ASV tables were randomly subsampled down to the minimum number of reads per sample of both rDNA sets (18,510 and 6,952 reads for the 16S and 18S rDNA sets, respectively) using the *rarefy* function in the vegan v2.5.7 package (Oksanen et al., 2021) in R v4.0.2 (R Development Core Team, 2021). The final ASV tables contained 55,530 rDNA 16S sequences clustered into 1,496 prokaryotic ASVs and 22,485 rDNA 18S sequences clustered into 920 protistan ASVs.

Metagenomic sequence assembly, gene prediction, and generation of a reference gene/peptide catalog

Metagenomic raw reads were trimmed for TruSeq adapters with cutadapt v1.16 and quality-filtered with trimmomatic v0.38 (Bolger et al., 2014) using the following parameters: LEADING:3 TRAILING:3 SLIDINGWINDOW:4:15 MINLEN:50. Metagenomic samples were then assembled using megahit v1.2.8 (Li et al., 2016) with meta-large preset and a minimum contig length of 500 bp. For each obtained metagenome, gene-coding sequences were predicted on the assembled contigs using Prodigal v2.6.3 (Hyatt et al., 2010). All 5,670,580 predicted coding sequences larger than 100 bp from each assembled metagenome were pooled and clustered at 95% sequence similarity and 90% sequence overlap of the smaller sequence using cd-hit-est v.4.8.1 (Li and Godzik, 2006) using the following options: -c 0.95 -T 0 -M 0 -G 0 -aS 0.9 -g 1 -r 1 -d 0 to obtain 4,779,650 non-redundant gene clusters.

Abundance and functional annotation of the reference gene catalog

The quality-checked sequencing reads of metagenomic samples were back-mapped against the nucleotide sequences of each gene cluster using Bowtie2 v2.3.4.1 (Langmead and Salzberg, 2012) with default options, keeping only mapping hits with quality >10 with Samtools v.1.8 (options: -q 10 -F 4) (Li et al., 2009). Read counts were reported for each metagenome using the HTSeq v0.10.0 (Anders et al., 2015) and the function htseq-count (options: -t CDS -r pos –nonunique all) to get the abundance of each of the 4,779,650 non-redundant gene clusters.

Identification and quantification of predicted DMSPC cycling genes

The amino acid sequences of predicted prokaryotic and eukaryotic DMSPC cycling genes (*Alma1*, *dsyB*, *DSYB*, *dddD*, *dddK*, *dddP*, *dddQ*, *dddW*, *dddL*, *dddY*, *dddX*, *dmdA*, *acuI*, *dmsA*/*torA*, and *tmm*; Table S2; Figure 3) were identified in the newly generated gene catalog. Reference phylogenetic trees were used for each of the genes to quantify their abundance as described below.

First, a collection of prokaryotic genome sequences was retrieved from the MAR databases (Klemetsen et al., 2018), the OceanDNA MAG catalog (Nishimura and Yoshizawa, 2022), and genome sequences reported in Paoli et al. (2022). This genome set contained all 1,270 complete genomes in the MAR databases and 5,521 partial genomes that had the "high quality" status as described in Klemetsen et al. (2018). All 52,325 OceanDNA genomes were included since they had been quality filtered based on their completeness and degree of contamination with the formula: percent completeness − 5 × percent-contamination ≥50. Only the genomes that passed this same quality filter were considered (Paoli et al., 2022), yielding another 26,942 genomes. A taxonomy was assigned to the genomes with the GTDB Toolkit (GTDB-Tk; Chaumeil et al., 2020). A smaller database was constructed for the products of the eukaryotic genes (*Alma1* and *DSYB*) (Table S2) in addition to all other possible algal peptides retrieved by BLASTp v2.12.0+ against GenBank and with the same predicted function.

To obtain the sequences for constructing the reference trees, the corresponding peptide for each gene was retrieved from the genome database with HMMER3 v3.3.2 (Eddy, 2008). In the case of the DMSO reductase, the search was based on hits to TIGR00509, which included DMSO reductase (DmsA) and trimethylamine-*N*-oxide reductase (TorA). As for acrylate catabolism, the peptides were annotated as AcuI if the gene was adjacent to *dmdA*, as observed in *Rhodobacteraceae* (Todd et al., 2012a) and the gene product belonged to the putative quinone oxidoreductase, YhdH/YhfP family (TIGR02823). Only *Rhodobacteraceae* AcuI peptides were considered since there was not a clear boundary between orthologs (enzymes with the same function) and paralogs (enzymes with a different function within the same protein family) for other taxa in the phylogenetic

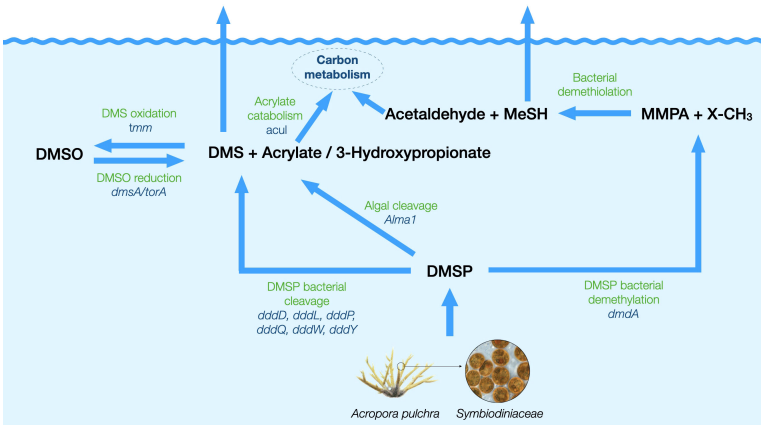

FIGURE 3
Schematic diagram of the putative pathways for the production and cycling of DMSP and derivatives around the studied *A. pulchra* colony, with the involved genes quantified in this study. DMSP is produced by the coral, the *Symbiodiniaceae*, and heterotrophic bacteria, and the target genes were *DSYB* for eukaryotes and *dsyB* for prokaryotes. DMSP is degraded into DMS and acrylate by its eukaryotic producers through the action of the *Alma1* gene, and also undergoes bacterial catabolism *via* multiple pathways: (i) bacterial demethylation into methylmercaptopropionate (MMPA), encoded by the gene *dmdA*, followed by demethiolation to methanethiol and acetaldehyde; (ii) bacterial cleavage into DMS and acrylate, targeted by the genes *dddP, dddL, dddQ, dddW*, and *dddY*; (iii) bacterial cleavage into DMS and 3-hydroxypropionate, encoded by the gene *dddD*. DMS oxidation to DMSO is encoded by *tmm*, and the reverse reduction is encoded by the DMSO/TMAO reductase gene (*dmsA/torA*). Acrylate is catabolized into the central carbon cycle, and one of the genes involved is *acuI*. Description and references of all these genes are given in Table S2.

reconstruction. For the remaining genes, since models (conserved domains in Table S2) retrieved the peptides of interest in addition to paralogs, hidden Markov models (HMMs) were designed to be specific for the gene products to quantify. Phylogenetic trees with peptides that shared the domains shown in Table S2 were used to select a subset with the predicted function. The selection of representative sequences for each gene as well as the boundary between orthologs and paralogs was based on the literature (Table S2). To select an HMM cutoff value, the highest e-value for the representative sequences for each gene when running the HMM profile was used as the highest e-value to do the searches in the peptides from the genome collection.

Reference phylogenetic trees were constructed with IQ-TREE v2.1.4-beta (Nguyen et al., 2015). The subclusters on each of the reference trees were labeled considering that their bootstrap values at the lowest nodes were above 70% and with a taxonomic rank common to all sequences within the subcluster. The reference trees were used to confirm that the taxonomy corresponded to the diversity described in the bibliography for each gene (Table S2).

To filter out most translated metagenome peptides that did not correspond to the function to quantify, first we did BLASTp searches of all metagenome peptides against each of the representative sets with a relaxed searching parameter (minimum bitscore of 50). The database to do the searches contained both the peptides from the reference trees for each gene and the rest of the peptides derived from the genome database, each with a proper label. Any metagenome peptide closer to the peptides on the reference trees was saved for the next annotation step. In case the reference sequences did not contain all diversity of peptides from each gene, an HMM search of the metagenome peptides was also carried out using the same HMM to retrieve the peptides to make the reference trees. Both hits with BLASTp and HMM searches were saved after removing duplicates between the two methods.

In a second step, the metagenome peptides that were retrieved before were placed on the reference trees. To do the placement, metagenome peptides were aligned with reference sequences using the package PaPaRa v2.5 (Berger and Stamatakis, 2011). A maximum likelihood placement was carried out with EPA-ng v0.3.8 (Barbera et al., 2019), with the amino acid substitution model predicted with IQ-TREE for the reference tree. Placed sequences with branch lengths longer than the longest distance between all pairs of sequences on the reference tree were removed (<1% of the sequences). Removed sequences were confirmed to correspond to a different function after performing BLASTp against the GenBank since closest sequences were classified with both Pfam or TIGRFAM in different protein families. At this step, <2% of the sequences had placements in subclusters with a different taxonomic label, although within the same higher rank in their taxonomy in most cases. From these multiple placements in the jplace files, for <1% of them, the sum of the "like weight ratio" that was shared with the best placement (highest "like weight ratio") was below 90%. Finally, the jplace file was converted into a newick text file using gappa v0.7.1 (Czech et al., 2020). The taxonomic assignments of the metagenome peptides in each group were confirmed after visualization of the placed sequences with iToL (Letunic and Bork, 2021).

For each DMSPC cycling gene, raw abundances of the identified peptide sequences were extracted from the gene abundance table previously obtained and normalized by gene size and sequencing depth using the transcripts per million (TPM) unit.

Results

Gradients of dissolved DMSPCs, VOCs, and microbes around reef-predominant organisms

Comparison of dissolved concentrations of DMSPCs and VOCs in the close vicinity of the organism colonies (0.5 cm, IN) and further away (2 m, OUT) was conducted to evaluate if three of the dominant organisms in the Mo'orea reefs were producers of these compounds (Figure 4).

A. pulchra *colonies*. Higher DMSPd concentrations (43–80 nM) were observed in seawater collected ~0.5 cm away from the coral (IN), 20- to 40-fold higher than OUT concentrations 2 m away (2 nM). A similar pattern was observed for DMS (12–50 nM *vs*. 1.3 nM), acrylate (18–65 nM *vs*. 2 nM), and DMSO (21–48 nM *vs*. 5 nM) (Figure 4). As for VOCs other than DMS, concentration gradients suggest that the *A. pulchra* holobiont produced the iodomethanes CH_3I (34–29 pM *vs*. 26–10 pM) and CH_2ClI (2.8 pM *vs*. 1.2 pM), yet the latter was only detectable around one of the colonies [AP(B)]. The only other VOC that showed some enrichment near the holobiont was COS (10–12 pM *vs*. 8–6 pM), whereas negligible differences were observed for dimethyl disulfide (DMDS), CS_2, isoprene, and bromomethanes (Figure 4). Likewise, no obvious differences were found in the prokaryotic and eukaryotic microbial abundances (Figure S1).

Pocillopora sp. *colonies*. Higher DMSPd concentrations were observed closest to this coral holobiont compared to 2 m away (2.2–6.8 nM IN *vs*. 0.8–1.3 nM OUT), although the concentration gradient was lower than observed for *A. pulchra* (Figure 4). However, the main difference from *A. pulchra* was the lack of a gradient for DMS (all approximately 1–2 nM) and DMSO (4.3–0.8 nM *vs*. 4.3–0.4 nM), and a weak gradient for

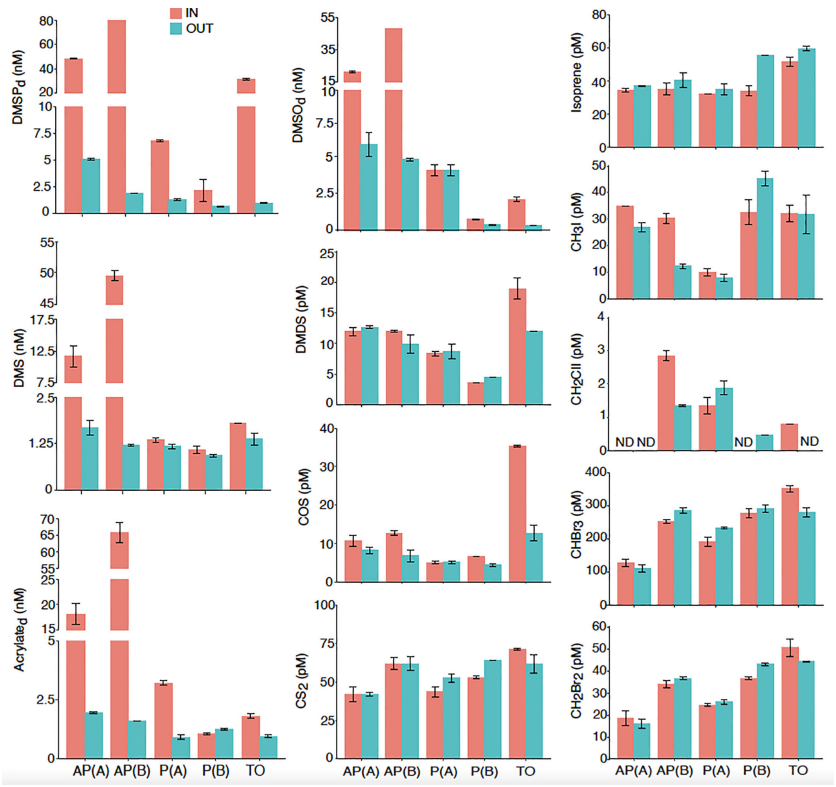

FIGURE 4
Dissolved DMSPC and VOC concentrations in the close vicinity (IN) and 2 m away (OUT) of two colonies of the coral *Acropora pulchra* [AP(A) and AP(B)], two colonies of the coral *Pocillopora* sp. [P(A) and P(B)], and a patch of the seaweed *Turbinaria ornata* (TO). Error bars denote the standard error of duplicate analyses. ND, not detected.

acrylate only observed on one occasion [3.3 nM *vs.* 1 nM in P(A), all ~1 nM in P(B)]. None of the measured VOCs, including DMS, showed enrichment in the inter-verrucae water of the *Pocillopora* sp. colonies, except for COS on one occasion [P(B)]. In most cases, the inter-verrucae water was slightly depleted in VOCs (Figure 4). As for microbial abundances, the only difference was with *Prochlorococcus*, which was more abundant close to the coral (Figure S1).

T. ornata *patch.* This seaweed showed enrichment in the closest sample for most sulfur compounds and halomethanes (Figure 4). The enrichment factor of DMSPd at 0.5 cm from the seaweed with respect to 2 m away was ~30 (31.5 nM IN *vs.* 1 nM OUT). Lower enrichments were observed for acrylate (1.8 nM *vs.* 1 nM), DMSO (2.3 nM *vs.* 0.4 nM), DMS (1.8 nM *vs.* 1.3 nM), and DMDS (19 pM *vs.* 12 pM). COS was the most enriched VOC near the seaweed (35 pM *vs.* 13 pM), and CS_2 was the least (70 pM *vs.* 60 pM). Higher concentrations closest to *T. ornata* were also observed for CH_2ClI (0.8 pM *vs.* not detected), $CHBr_3$ (352 pM *vs.* 280 pM), and CH_2Br_2 (50 pM *vs.* 44 pM). Isoprene and CH_3I showed no enrichment (Figure 4). Among microbes, only *Prochlorococcus* was more abundant close to the seaweed (Figure S1).

Diel cycle of DMSPCs, VOCs, and microorganisms around an *A. pulchra* colony

Here, an *A. pulchra* colony was sampled every 6 h throughout an entire day/night cycle, at three sampling points: between the living branches, ~0.5 cm next to the polyps (IN); deeper between the branches, ~0.5 cm next to the turf alga that colonizes the dead coral (AL); and 2 m down current from the colony patch in seawater overlaying a sandy bottom (OUT). DMSPC and VOC concentrations are shown in Figure 5.

DMSPCs. For the diel study, both the dissolved and total (dissolved + particulate) pools of non-volatile DMSPCs were measured (Figure 5). DMSP was 17%–65% dissolved in IN, 8%–50% in OUT, and 13%–29% in AL. Acrylate was 66%–90% dissolved in IN, 60%–94% in OUT, and 13%–57% in AL. DMSO was 88%–98% dissolved in IN, 93%–100% in OUT, and 29%–92% in AL. Again, DMSPC concentrations were much higher nearest the tips of the branches (IN), where live polyps were present, compared to the concentrations 2 m away (OUT). This was valid for both the dissolved and the total pools of DMSP, acrylate, and DMSO, as well as for DMS. The most salient

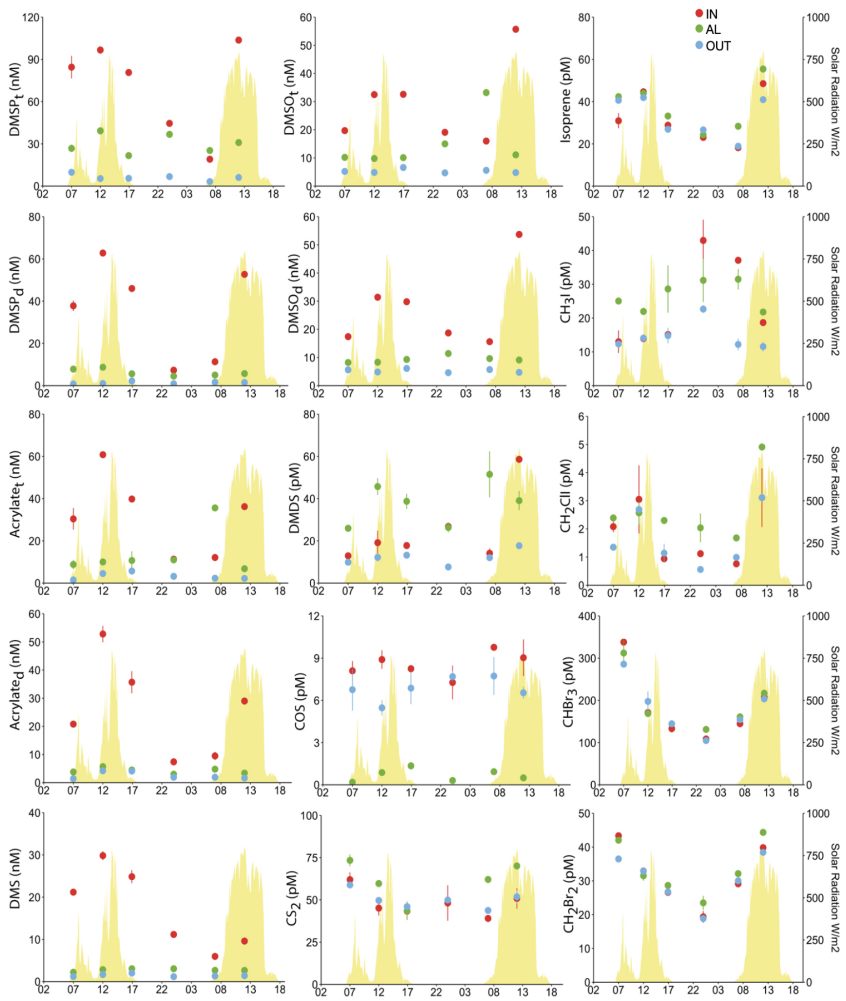

FIGURE 5
Total and dissolved DMSPC concentrations, and VOC concentrations around an *Acropora pulchra* colony over a diel cycle. Seawater samples were taken in the close vicinity of the living branch tips occupied by polyps (IN), the dead base of the branches, colonized by turf algae (AL), and 2 m away from the colony over a sandy bottom (OUT). Error bars denote the standard error of duplicate analyses. The yellow peaks in the background depict total solar radiation.

feature was the strong diel pattern in IN, with highest concentrations around local noon and lowest at late night (Figure 5). The pattern was very consistent across the four DMSPCs, pointing to common causes. Strikingly, in all cases and particularly at midday, concentrations dropped dramatically between IN and AL, which were only 10 cm apart (Figure 5). Not only were the concentrations lower, but no diel pattern was seen in AL. The lowest DMSPC concentrations were found in the seawater out of the coral patch, but it is noteworthy that there was greater similarity, in both concentrations and temporal trends, between AL and OUT (2 m) than between IN and AL (10 cm) (Figure 5). In other words, similarities were not related to distance.

VOCs. DMDS, which also has its putative origin in DMSP (see below), exhibited a diel pattern that roughly paralleled that of the DMSPC (increase at midday, decrease towards a minimum at late night), but its spatial distribution was totally distinct, with generally AL > IN > OUT (Figure 5). CS_2 concentration was also higher in AL during the day and indistinguishable among the three sampling points during the night (Figure 5). In contrast, the most volatile sulfur compound, COS, was similar in IN and OUT, without a clear diel pattern, but was greatly depleted in AL. Isoprene showed a very clear diurnal enhancement but without any spatial gradient. The pattern of CH_3I was opposite to those of most VOCs, with the maximum around midnight and the minimum at midday. The largest amplitude of this variation was observed in IN, and the smallest amplitude but generally higher concentrations were observed in AL. CH_2ClI concentrations clearly followed the sunlight cycle, and were generally higher in AL. Finally, the two

bromomethanes $CHBr_3$ and CH_2Br_2 did not exhibit spatial gradients but their diel cycle showed strong variability towards a minimum at midnight and increasing into the day (Figure 5).

Microbial abundances. In general, there were higher abundances of heterotrophic prokaryotes, *Prochlorococcus*, and autotrophic pico- and nanoeukaryotes in AL, while IN and OUT were only distinguishable because IN harbored higher densities of high nucleic acid containing bacteria (HNA-Bact) (Figure 6). The temporal variation was generally parallel across sampling points: bacteria showed a bimodal pattern with abundance maxima at midday and midnight. Phytoplankton showed a clear maximum, indicating concerted cell division, at midnight. The exception was *Synechococcus*, which showed no differences among sampling points and cell division in the afternoon towards the dusk (Figure 6).

Fine spatial distribution of microbial community composition and diversity around an *A. pulchra* colony

At noon of the second day of our diel survey, coinciding with maximum DMSPC concentrations around the coral colony, we collected extra water volume to investigate the microbial diversity by rDNA amplicon sequencing. A total of 1,496 prokaryotic and 920 eukaryotic ASVs were retrieved among the three sampling points IN, AL, and OUT (Figures 7A, B). Rarefaction curves leveled off for both 16S and 18S rDNA sets, suggesting that most microbial diversity was sequenced in each sample (Figure S2). For prokaryotes, the highest diversity was retrieved in AL: 924 ASVs (~62% of the total), 40% of which were specific to this sample (Figure 7A and Table S3). In the case of eukaryotes, the highest protistan diversity was retrieved in OUT, with a total of 735 ASVs (~80% of the total), of which up to half were only retrieved in this sample (Figure 7B and Table S3). Interestingly, the community richness of prokaryotes and protists, although relatively high in both cases, showed an opposite trend across samples, as indicated by the S_{Chao1} and Shannon diversity indices (Figure S2). Indeed, the most and least diverse prokaryotic communities occurred in AL (H' = 6) and OUT (H' = 4), respectively, while the opposite trend was seen for the protistan community (H' = 4.1 in AL and H' = 5.6 in OUT).

Overall, only small fractions of the prokaryotic (13%) and eukaryotic (5%) microbial diversities were shared between the three samples (Figures 7A, B). Pairwise comparisons of the community composition (Table S3) showed the highest similarity between IN and OUT for prokaryotes ($S_{Sørensen}$ = 0.58, S_{BC} = 0.68), and to a lesser extent also for protists ($S_{Sørensen}$ = 0.46, S_{BC} = 0.38). Both IN and OUT were relatively dissimilar to AL in their prokaryotic and eukaryotic composition ($S_{Sørensen}$ < 0.35, S_{BC} < 0.25). Consequently, the IN and OUT microbial communities shared up to 25% of their diversities despite being the most distant. The nearest communities (IN and AL, only 10 cm apart) had fewer taxa in common, only 7% of the protistan ASVs.

Given the low proportion of microbial diversity shared between samples and the singularity of AL, we explored if similar differences could be observed at the genus taxonomic level as a microbial food web descriptor (Figures 7C, D). We observed dissimilarities in cyanobacteria obtained by amplicon sequencing (Figure S3). As much as 32% and 44% of the prokaryotic community was constituted by cyanobacterial sequences in IN and OUT samples, respectively, while this proportion fell to <4% in AL. The two most abundant cyanobacteria genera were *Synechococcus*, predominant in OUT, and *Prochlorococcus*, with increased presence at IN (Figure 6). As

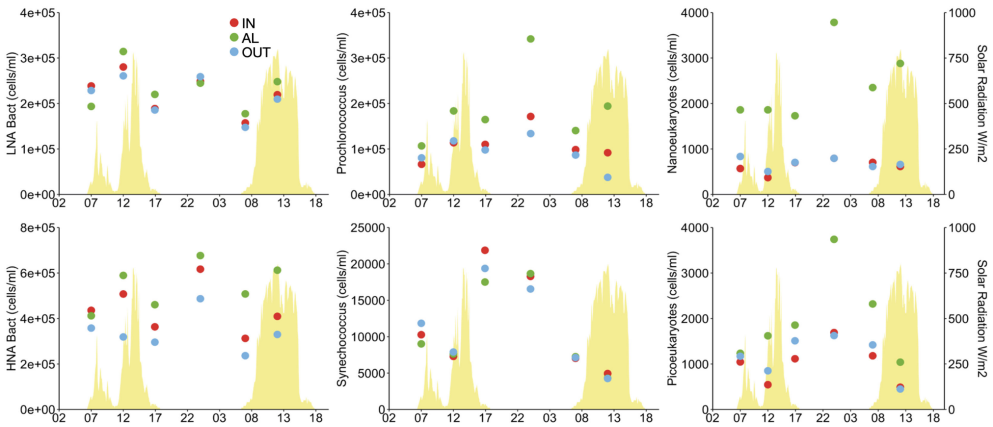

FIGURE 6
Microorganism abundances around an *Acropora pulchra* colony over a diel cycle as determined by flow cytometry. Details of where samples were collected are given in Figure 5. HNA, high nucleic acid containing heterotrophic prokaryotes; LNA, low nucleic acid containing heterotrophic prokaryotes.

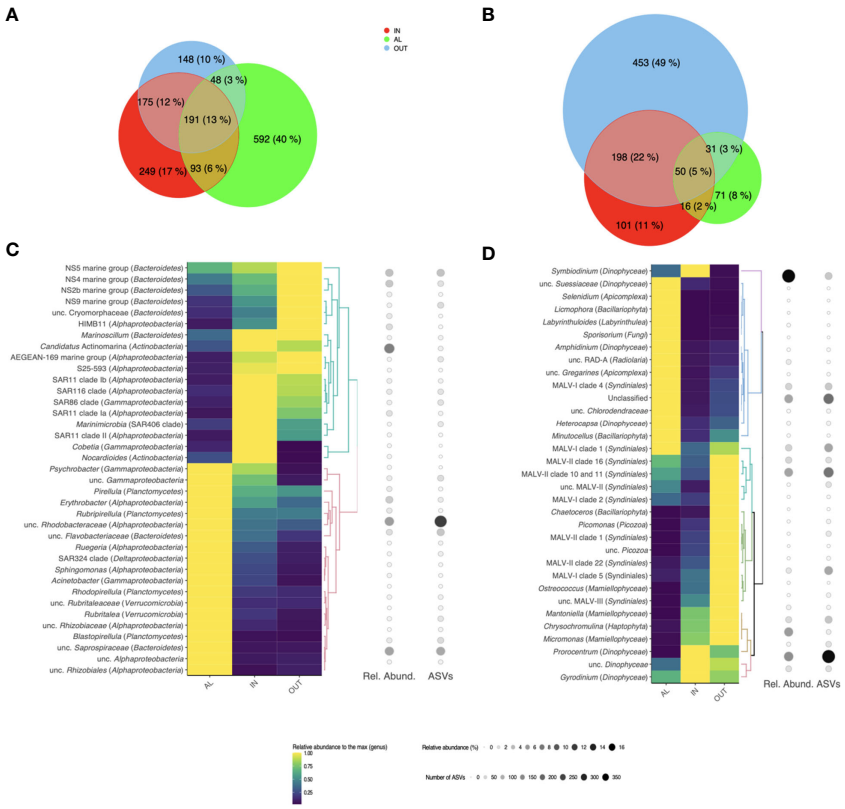

FIGURE 7
Microbial diversity and composition around an *Acropora pulchra* colony. Venn diagrams show the shared and unique amplicon sequencing variants (ASVs) between the heterotrophic bacterial **(A)** and protistan **(B)** communities in samples IN, AL and OUT collected on 25 April 2018 at local noon. Below the number of shared/unique ASVs, the percentages of the total richness they represent are indicated. Heatmaps display the distribution of the main bacterial **(C)** and protistan **(D)** genera in the samples. Only genera that are dominant in at least one of the three samples (representing more than 1% of the total reads in this sample) are showcased, and their relative abundances are scaled to the maximum relative abundance retrieved among the three samples. For each genus, its relative abundance (number of sequences) and richness (number of different ASVs) within the whole sequencing dataset are also indicated.

for the heterotrophic prokaryotic community (Figure 7C), the marine genera of the *Bacteroidetes* phylum (NS2b, NS4, NS5, and NS9 marine groups) and the alphaproteobacterial strain HIMB11 (*Rhodobacteraceae*) were dominant in OUT, while the bacterioplankton in IN were dominated by the ubiquitous alphaproteobacterial clades SAR11, SAR86, and SAR116, known oligotrophs, as well as coral reef characteristic bacteria such as *Candidatus* Actinomarina (Apprill et al., 2016) and *Marinoscillum* (Seo et al., 2009). The bacterioplankton composition in AL was indeed distinct, with abundant sequences affiliated to unclassified *Rhodobacteraceae* and *Flavobacteriaceae*, and to the gammaproteobacterial *Acinetobacter*, known to have copiotrophic lifestyle (Fuhrman et al., 2015). We also retrieved sequences affiliated to putative epiphytic bacteria, such as *Planctomycetes* (*Pirellula* spp. and *Rubripirellula* spp.) and *Verrucomicrobia*.

Regarding the protistan community (Figure 7D), there was a clear dominance of sequences affiliated to *Dinophyta* (i.e., *Dinophyceae* and *Syndiniales*) in the three samples. The overrepresentation of sequences affiliated to dinoflagellates in amplicon datasets is a well-known feature (e.g., Koid et al., 2012; Gong et al., 2015). It is mostly explained by the large variation in the ribosomal (r)DNA operon copy number across protist taxa, which can reach out several thousands in some dinoflagellates or ciliates (Zhu et al., 2005; Vd'acný et al., 2011). Yet, our results show a high prevalence of sequences affiliated to *Symbiodiniaceae* in IN, next to the polyps of *A. pulchra*, suggesting the release of algal symbionts to the surrounding environment, a process known to occur on a daily basis (Broadbent and Jones, 2006). Outside the colony patch (OUT), the eukaryotic community was dominated by sequences affiliated to *Mamiellales* (*Micromonas* spp. and *Mantoniella* spp.), *Haptophyta* (*Chysochromulina* spp.), and *Syndiniales* (parasitic dinoflagellates). Lastly, in AL, we retrieved sequences of *Labyrinthuloides*, organisms responsible for the decomposition of both allochthonous and autochthonous

organic matter (Collado-Mercado et al., 2010). This confirmed the unique environment around the turf alga at the base of the coral branches, where algal-derived organic matter favors the development of copiotrophs.

Quantification of functional genes for DMSPC cycling around an *A. pulchra* colony

At noon of the second day of the diel cycle, a number of target genes encoding for DMSPC transformations (Figure 3) were detected around the *A. pulchra* colony, including those encoding for DMSP biosynthesis (*dsyB* and *DSYB*), demethylation (*dmdA*), and cleavage (*Alma1* and *ddd*-), DMS oxidation (*tmm*), DMSO/TMAO reduction (*dmsA*/*torA*), and one of the possible routes of acrylate catabolism (*acuI*). When the IN and OUT samples were considered together, *dmdA* (widely distributed but mostly in SAR11, *Rhodobacteraceae*, and other *Alphaproteobacteria*) and *tmm* (also mostly in SAR11 and *Rhodobacteraceae*) were the most abundant among the target prokaryotic genes, followed by *dddP* (*Rhodobacteraceae* and SAR116) and *dddQ* (*Alphaproteobacteria*). No significant differences were apparent between IN and OUT except for the DMS production gene *dddD* (Figures 8A–C), which showed enrichment in IN by nearly a factor of 20 (Figure 8B). These sequences clustered with DddD peptides in *Endozoicomonas*, a genus of *Gammaproteobacteria* that dominates the coral microbiome across a wide range of coral species (Bourne et al., 2016) and can grow on DMSP as the sole carbon source (Tandon et al., 2020). Sequences of *dddD* in OUT were classified instead in the family *Litoricolaceae* (*Gammaproteobacteria*). Neither the gene for bacterial DMSP biosynthesis *dsyB* (alphaproteobacterial) nor the genes for DMSO reduction (alphaproteobacterial) and acrylate catabolism *acuI* (*Rhodobacteraceae*) showed any difference in relative abundance between IN and OUT (Figure 8B).

The gene encoding for the DSMP lyase, *Alma1*, was the most abundant of the three target eukaryotic genes, followed by the homolog to the prokaryotic *tmm*, and *DSYB* (Figures 8A, B). *Alma1* and *tmm*, likely associated with *Acropora* and *Symbiodiniaceae*, were found in IN and undetectable in OUT.

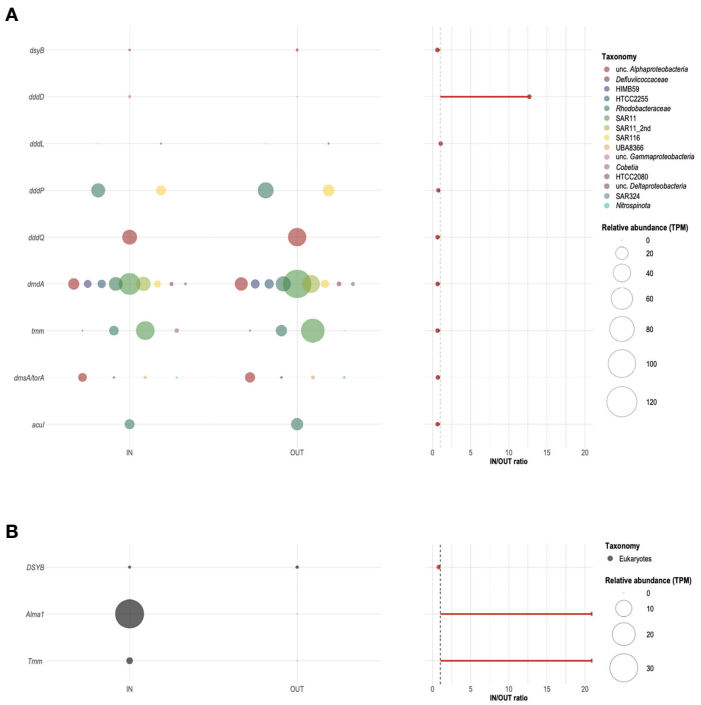

FIGURE 8
Relative abundance and taxonomic profiling of potential bacterial **(A)** and eukaryotic **(B)** DMSPC-cycling genes around an *Acropora pulchra* colony. Bubble plots on the left show the relative abundance, expressed in transcript per million (TPM) of target genes (*dsyB*, *DSYB*, *Alma1*, *dddD*, *dddL*, *dddP*, *dddQ*, *dmdA*, *tmm*, *dmsA*/*torA*, and *acuI*) identified in samples IN and OUT collected on 25 April 2018 at local noon. The colors of the bubbles indicate their taxonomic assignment. No sequences related to genes *dddK*, *dddW*, *dddY*, or *dddX* were detected in our metagenomes. The IN/OUT ratio of the relative abundance of each of the target genes is shown on the right. The dashed gray line corresponds to a ratio equal to 1.

Discussion

Sources of DMSPCs and VOCs

Concentration gradients in close proximity to three of the dominant benthic organisms in the reefs (Donovan et al., 2020) provided valuable information about the VOC and DMSPC sources (Figures 4, 5). *A. pulchra* was confirmed to be a strong source of all DMSPCs (DMSP, DMS, acrylate, and DMSO). Coral holobionts of the genus *Acropora* are well known for being DMSP producers and releasing products of DMSP catabolism (Tapiolas et al., 2010; Raina et al., 2013; Tandon et al., 2020; Guibert et al., 2020). DMS and acrylate were the only catabolic products that showed an increase near the polyps that paralleled the increase of DMSPd, indicating that DMSP-lyase-mediated DMSP cleavage was important, either by the coral itself, the algal symbiont (*Symbiodiniaceae*), or associated bacteria (see below). No significant gradient of DMDS was observed. This compound is very rarely measured in seawater; we interpret its occurrence in the Mo'orean reef sample chromatograms as a reflection of the presence of methanethiol (MeSH). It has been reported that high temperatures and activated carbon, two characteristics of our purge and trap system prior to GC injection and analysis, can oxidize MeSH to DMDS (Cheng et al., 2007). The absence of a gradient of DMDS from *A. pulchra* suggests that DMSP cleavage prevailed over the demethylation + demethiolation pathway (Figure 3; Landa et al., 2019) in DMSP catabolism. Much less is known about DMSO production and release by corals; our results point to DMSO resulting from DMS oxidation (photochemical or microbial) inside the coral holobiont. According to VOC gradients, *A. pulchra* was not a significant source of VOC other than DMS, except for a little COS, which might be related also to DMS photo-oxidation (Lennartz et al., 2020), and iodomethanes, which likely originated in the turf algae that covered the coral skeleton (see below).

Pocillopora sp. was also a source of DMSPd, yet the DMSPd concentrations between the verrucae were 6- to 40-fold lower than between the branches of *A. pulchra*. *Pocillopora* sp. corals are known to produce and release copious amounts of DMSP in connection to oxidative stress. Released DMSP, particularly when it accumulates in the mucus of stressed colonies, may elicit chemoattraction of pathogenic bacteria (Garren et al., 2014). Despite DMSP release, *Pocillopora* sp. was a weak source of DMS, acrylate, and DMSO (Figure 4). This is consistent with Exton et al. (2015) and Lawson et al. (2021), both of whom did not detect DMS in *Pocillopora* corals. We show that *Pocillopora* sp. does produce DMSP but probably does not harbor high DMSP-lyase activity for significant cleavage in the holobiont. This coral also did not produce any VOCs other than DMS, except for a little COS again, probably resulting from the photo-oxidation of DMS.

The seaweed *T. ornata* was a strong source of DMSP, but less so for DMS, acrylate, and DMSO. Burdett et al. (2013) already reported that intracellular DMSP makes up to 0.4% of the weight of a *Turbinaria* sp. from a tropical reef. Like *Pocillopora* sp., neither this seaweed nor its epiphytic bacteria seem to harbor DMSP lyases. This is further supported by the significant increase of DMDS (MeSH) towards the alga; instead of cleavage, released DMSP underwent degradation through demethylation (Figure 3). Since DMSP degradation with MeSH production is only known in prokaryotes, this process was probably conducted by epiphytic bacteria. The seaweed was also a strong source of COS; as with the corals, COS could result from DMS photo-oxidation, but it could also result from photochemical reactions on the seaweed-derived organic matter (Cutter et al., 2004). Other VOCs that were enriched near *T. ornata* were the halomethanes CH_2ClI, $CHBr_3$, and CH_2Br_2. Many macroalgae, including tropical seaweeds and including the genus *Turbinaria*, are known producers of halocarbons, particularly $CHBr_3$ (Leedham et al., 2013; Lim et al., 2017). Suggested physiological and ecological functions are oxidative-stress mitigation (Goodwin et al., 1997; Abrahamsson et al., 2003) and chemical defense against parasitic microbes (Ohsawa et al., 2001). Given that bromomethanes only showed positive gradients towards *T. ornata* and not to the corals, we suggest that the high levels of bromomethanes in the Mo'orean reefs are attributed to the large abundance of macroalgae, among which *T. ornata* dominates.

Are the Mo'orean reefs hotspots of VOC production?

Tropical coral reefs are suggested to be hotspots of VOC production (Exton et al., 2015) because of the high density and diversity of organisms, with presumably large needs for chemical interactions, and their exposure to natural physiological stressors such as high solar irradiance and temperature, water-column transparency to UV radiation, and low nutrient concentrations. Even though we did not characterize anything close to the entire volatilome in the Mo'orea coral reefs, our target VOCs were chemically diverse enough to provide insight into the "VOC hotspot" hypothesis.

In the two reef sites studied here, the OUT seawater samples taken 2 m away from reef-dominant organisms, generally over sandy floor, can be regarded as background waters from inside the reef lagoon that gather VOC contributions from all reef components (Figures 4, 5). Isoprene occurred in the 20–60 pM range, very similar to the range reported for ocean tropical waters outside the regions of equatorial upwelling (Dani and Loreto, 2017). COS ranged between 4 and 11 pM, a little lower than most of the measurements in the tropical ocean (10–20 pM; Lennartz et al., 2020). CS_2 was 40–60 pM, much higher than in most tropical ocean waters (5–15; Lennartz et al., 2020). The range of CH_3I concentrations in reef waters (8–45 pM) was higher than typical concentrations in tropical open waters (1–10 pM; Ziska et al., 2013). We measured very low concentrations of CH_2ClI (ND-3 pM), similar to the 1–3 pM reported by Ooki

et al. (2015) in non-upwelling tropical ocean waters. As for bromomethanes, concentrations in the Mo'orean reefs were 30- to 100-fold higher than those in non-coastal tropical waters in the case of $CHBr_3$ (100–300 pM *vs*. 1-8 pM), and 6- to 15-fold in the case of CH_2Br_2 (15–45 pM *vs*. 1–8 pM; Ziska et al., 2013). DMS concentrations were 1–1.3 nM, in the lower range of tropical open ocean levels (1–5 nM; Lana et al., 2011). We also detected DMDS at concentrations within the 5–15 pM range, which putatively correspond to MeSH concentrations of 10–30 pM, since 1 mol of DMDS corresponds to 2 mol of MeSH. Actually, very few measurements of oceanic MeSH exist because its high reactivity to surfaces makes its analysis challenging. From the few reported measurements, Kettle et al. (2001) estimated that the DMS : MeSH concentration ratio across the Atlantic was 1–30, with a mean of 5–6. We do not know if MeSH was totally converted to DMDS in our system, probably not because the average DMS : DMDS ratio was around 100 (i.e., the putative DMS : MeSH ratio was 50), but DMDS variability can be considered a good proxy of MeSH variability. Overall, the studied reef waters were rich only in CS_2, CH_3I, and particularly $CHBr_3$ and CH_2Br_2, when compared to the average tropical ocean.

DMSP-derived compounds (DMSPCs) other than DMS (namely, DMSP, acrylate, and DMSO) occurred at rather low dissolved concentrations 2 m away from the studied organisms. In the Mo'orean reef lagoon, DMSPd (1–5 nM) and DMSOd (0.5–6 nM) were four to six times lower than in the Great Barrier Reef. No similar data exist with which to compare our dissolved acrylate concentrations (1–3 nM). Plausible reasons for lower DMSPC in Mo'orea are as follows: (i) the fact that corals are not exposed to air and the consequent stress, (ii) differences in the dominant coral species, and (iii) differences in the filtration method (Xue et al., 2022). Furthermore, microbial consumption rates of DMSPd and acrylate in the Mo'orean reefs were faster than most reported rates from any site (Xue et al., 2022), yet there are no data from the Great Barrier Reef to compare with.

Are DMSPC and VOC patterns consistent with a role in coping with light-derived oxidative stress in *A. pulchra*?

Many studies have addressed how corals cope with environmental stress, including the exposure to high irradiance (e.g., Schrameyer et al., 2016; Nitschke et al., 2018). However, to our knowledge, only one study has looked at DMSPC production by a coral over an entire diel cycle (Broadbent and Jones, 2006), and no study has considered VOCs.

Over the diel cycle around the *A. pulchra* colony at the Tema'e Beach reef, both total and dissolved DMSPCs were much higher, closest to the coral polyps, where they largely increased towards noon and decreased towards midnight, following the pattern of solar radiation. Corals of the genus *Acropora* are known to increase their internal DMSP and/or DMSO concentrations in response to stress caused by high irradiance, risen temperatures, hyposaline events, or exposure to air at low tide (Raina et al., 2013; Deschaseaux et al., 2014b; Gardner et al., 2016; Hopkins et al., 2016). Upregulation of DMSP production and turnover can be contributed by the major holobiont components in which the capacity for DMSP biosynthesis has been described: the cnidarian host (Raina et al., 2013), the *Symbiodiniaceae* algal symbiont (Deschaseaux et al., 2014a), and the coral- and *Symbiodiniaceae*-associated bacteria (Curson et al., 2017; Lawson et al., 2020; Kuek et al., 2022). The breakdown of DMSP into DMS and acrylate is suggested to be a mechanism of the coral holobiont to alleviate oxidative stress (Raina et al., 2009), as indicated by previous studies of coral tissue and mucus (e.g., Hill et al., 1995; Broadbent et al., 2002; Raina et al., 2013; Swan et al., 2017; Haydon et al., 2018), since both DMS and acrylate may act as reactive oxygen species (ROS) scavengers (Tapiolas et al., 2010). The cnidarian *Acropora millepora* and several *Symbiodiniaceae* clades have been found to harbor the eukaryotic DMSP lyase Alma1 (Alcolombri et al., 2015), consistent with demonstrated DMSP cleavage activity (Yost and Mitchelmore, 2009). Coral-associated bacteria harbor prokaryotic DMSP lyases too (Raina et al., 2009).

Indeed, the data displayed in Figures 5, 7, and 8 support the light stress hypothesis. DMSPC concentrations in seawater next to the polyps (IN) increased with light, and the pools that increased the most were the dissolved forms. In the last time point of the diel series, at noon, the IN : OUT enrichment factors of 10–50 for dissolved DMSPCs contrasted with the fact that the prokaryotic microbial assemblage composition in IN and OUT was not that different (41% of shared ASVs), suggesting that the light-triggered DMSPCs were mainly released by the coral holobiont. All the target genes in the DMSPC cycle showed same specific abundances right next to the coral and 2-m down current, except for the eukaryotic DMSP cleavage gene (*Alma1*), the eukaryotic DMS oxidation gene (*tmm*), and the prokaryotic DMSP cleavage gene *dddD*. This points to a limited role of reef free-living bacteria to explain the diurnal pulses in DMS, acrylate, and DMSO near the coral. Even though free-living bacteria did not control these pulses, they were nonetheless tuned into daily inputs, as discussed in a companion paper (Xue et al., 2022). The diel trend in DMSPC concentrations paralleled the trend in the microbial uptake of dissolved acrylate and DMSP, with uptake rate constants higher during the day and lower at night, and turnover times on the order of hours. This suggests that the free-living microbial community was well attuned to diel changes in these substrates originating from the coral.

The observation that DMDS (MeSH) showed almost no gradient towards the coral is consistent with the observation that *dmdA* was not enriched in the bacteria closest to the coral tips, and confirms that the coral holobiont did not degrade most of its

DMSP through the sulfur-assimilative demethylation route but through cleavage. Non-cleaved DMSPd was dispersed by the flow and fed bacterial consumption along the reef lagoon (Xue et al., 2022). In contrast, DMDS (MeSH) concentrations were higher near the turf alga (AL) despite DMSPd concentrations that were much lower, indicating that a larger share of DMSP was demethylated. Unfortunately, we could not quantify functional genes in sample AL and hence we could not confirm that *dmdA* was enriched near the turf alga, but the presence of epiphytic and copiotrophic bacterial taxa (Figure 7) suggests higher bacterial activity, larger carbon and sulfur demands, and greater DMSP–sulfur assimilation.

Regarding VOCs other than DMS and DMDS, isoprene increased during the day and decreased at night. This pattern was expected, since isoprene is a photosynthesis-related compound proposed to be used by vascular plants and phytoplankton to combat thermal and oxidative stress (Meskhidze et al., 2015; Dani and Loreto, 2017; McGenity et al., 2018). In *Acropora* corals, Swan et al. (2016), Lawson et al. (2021) and Dawson et al. (2021) reported isoprene production by *A. aspera*, *A. intermedia*, and *A. horrida*, respectively. However, while *A. aspera* increased isoprene production when subject to stress and mucus release by shaking, and *A. horrida* behaved similarly upon temperature increase, no difference was observed in isoprene production by *A. intermedia* under heat stress. Since cultured *Symbiodiniaceae* produce isoprene (Exton et al., 2013), it is not known if the previously reported production by *Acropora* spp. holobionts is to be attributed only to the algal symbionts or to the cnidarian host as well. We did not find significant differences in the concentrations or diel pattern of isoprene concentration between the three sampling points, which indicates that the *A. pulchra* colony was not the source of this compound but rather the surrounding phytoplankton were responsible for sunlight-enhanced isoprene production in our reef.

Other VOCs that were expected to increase during daytime around *A. pulchra* were COS and CS_2, two products of amino acid, DMS, and organic matter photochemistry (Xie et al., 1998; Lennartz et al., 2020), with a release potential from the coral holobiont. The absence of a clear diel pattern of COS and the absence of a gradient with distance from the coral indicate that *A. pulchra* neither produced COS nor favored its production. The salient COS depletion near the turf alga on the dead coralline skeleton (AL), likely an organic matter-rich microhabitat, points to either enhanced hydrolysis (Elliott et al., 1987) or algal uptake (Blezinger et al., 2000) as local COS sinks. CS_2 showed the expected diel pattern but no gradient with distance from the coral tips, indicating no production by *A. pulchra*. Instead, it was higher near the turf alga, due to either organic matter photochemistry or production by increased phytoplankton numbers (Figure 6; Xie et al., 1999).

As for the iodomethanes, CH_3I concentration peaked at midnight. Therefore, the predominant CH_3I source around *A. pulchra* was not photochemical (Richter and Wallace, 2004) but biological (Yokouchi et al., 2014). Over most of the diel cycle, CH_3I was enriched near the turf alga on the dead branches, and only at midnight was it higher nearest to the coral tips. Thus, it is hard to say if CH_3I originated in the coral holobiont, the turf alga, or phytoplankton (which doubled at midnight, Figure 6). It was probably all of them. In contrast, the clear diel pattern of CH_2ClI points to light-related production. As a polyhalogenated compound, it could have resulted from the action of haloperoxidases (in this case, iodoperoxidases) used by organisms to alleviate hydrogen peroxide-induced stress under high sunlight (Moore et al., 1996). CH_2ClI concentrations were generally higher near the turf alga, with no clear evidence of production by the coral holobiont.

Similar to CH_2ClI, the two target poly-bromomethanes likely originated from the action of bromoperoxidases to scavenge harmful hydrogen peroxide (Moore et al., 1996). $CHBr_3$ and CH_2Br_2 exhibited parallel diel patterns with increasing concentrations during the day. The absence of spatial gradients towards the *A. pulchra* tips or the skeleton covered by the turf alga further supports that the main source was not the coral colony but the abundant seaweeds across the reef, particularly *T. ornata*.

Even though most of the target VOCs are regulated by sunlight-related chemical and biological processes, and several are likely involved in oxidative stress alleviation, no VOC except for DMS showed patterns consistent with being released by the *A. pulchra* holobiont to alleviate oxidative stress. In contrast to VOC, the distribution and diel pattern of DMSPC were compatible with their role as holobiont's antioxidants or, at least, their release as a consequence of oxidative stress.

DMSPC release and algal symbiont expulsion at high light

A detailed look at Figure 5 reveals that not only dissolved DMSPCs increased closest to *A. pulchra* during the day, but also particulate DMSP (DMSPp = DMSPt – DMSPd). The characteristics of the eukaryotic microbial assemblage (as defined by the 18S rDNA amplicons) near the coral at noon provided clues to the identity of the microorganisms this DMSPp belonged to: symbiodiniacean ASVs were heavily enriched in IN compared to OUT samples (Figure 7). The higher IN abundance of *Symbiodiniaceae* ASVs could explain the higher DMSPp concentrations near the polyps. Reinforcing this idea, two eukaryotic genes (*Alma1* and *tmm*) were among the few genes only found in IN. The closest archived sequences of these genes belong in *Acropora* and symbiodiniacean genomes (data not shown). The presence of *Acropora* genes can be explained by the release of DNA to the surrounding seawater as part of the extracellular DNA pool (eDNA; Kutti et al., 2020); the presence of symbiodiniacean genes can be explained by symbiont expulsion from the holobiont.

Expulsion of *Symbiodiniaceae* from the polyps into the surrounding seawater is a common process in corals (Hoegh-Guldberg et al., 1987). It occurs mostly around midday, typically associated with mucus release, and is thought to be a response to thermal and sunlight-derived oxidative stress when photo-inhibition and damage by ROS overcome protection in the algal symbiont (Weis, 2008; Curran and Barnard, 2021). We speculate that, in our study case in the shallow Tema'e Beach back reef, *A. pulchra* would expel symbionts as solar radiation increased, along with their associated high DMSPp content. As the expelled *Symbiodiniaceae* would be the most damaged by oxidative or thermal stress (Fujise et al., 2014), before and after expulsion they would transform part of their DMSP into DMS, acrylate, and DMSO (Sunda et al., 2002; Galí et al., 2013; Deschaseaux et al., 2014a). The absence of a thick mucus layer would facilitate the rapid dispersal and dilution of non-cleaved DMSPd by the fast flow, which made it available to reef lagoon bacteria and phytoplankton.

The higher relative abundance of the prokaryotic gene *dddD* near the polyps can also be explained by release from the coral holobiont. Interestingly, Raina et al. (2009) reported that bacteria isolated from coral tissue by enrichment with DMSP showed the presence of DddD and DddL as the only DMSP-degrading enzymes. In our metagenomes, *dddD* belonged entirely to *Gammaproteobacteria*, particularly to *Endozoicomonas* in the sample closest to the polyps. *Endozoicomonas* are ubiquitous endosymbionts in corals, predominant in coral tissues (Bourne et al., 2016). There is no evidence they are associated with *Symbiodiniaceae* (Maire et al., 2021) and can therefore be expelled together, but they are commonly found in the ecosphere around corals (Weber et al., 2019). Indeed, we detected *Endozoicomonas* ASVs only in sample IN, yet at relative abundance <1%.

What do VOCs, DMSPCs, microbial diversity, and gene abundances suggest about water flow, hydrodynamic layers, and connectivity in a branched-coral colony?

It has been long suggested that coral holobionts, by release of organics including DMSPCs, may shape the microbiome within and around them (Raina et al., 2010). This is clear inside the coral, as well as outside when there is a mucus layer, and since the mucus gets enriched in labile organics, symbiodiniacean cells, and associated bacteria, it is retained for a while next to the coral (as it offers viscous resistance to turbulent diffusion or advection by the flow), allowing local microbial growth, and may thus sustain a distinct microbial community. The mucus layer may also attract chemotactic microbes from the surrounding seawater (Garren et al., 2014). However, beyond the mucus layer, the strong flow across highly branched corals will prevent the buildup of a distinct microbiome in the waters next to the coral, except for those microbes released by the coral itself, which will rapidly dilute into the reef water.

In our *A. pulchra* colony, which was never exposed to the air and did not produce a visibly copious mucus, the taxonomic diversity of the microbial communities and their DMSPC-cycling gene inventory suggest a high connectivity between the coral tips and the surrounding waters (Figures 2, 7, 8). The chemical, taxonomic, and genetic differences between the waters next to the coral polyps (IN) and down current (OUT) can be explained by direct release from the coral holobiont. The most striking feature is that the sample AL, located only 10 cm below IN, was the most dissimilar of the three. Here, there could also be a constant release of epiphytic and endosymbiotic microbes from the turf alga, but the only explanation for the buildup of such a distinct community with respect to IN is that the connectivity between the two is dramatically reduced. This lack of connectivity can be explained by invoking the fine hydrodynamics of coral knolls (Shashar et al., 1996). While IN was located within the "outer benthic boundary layer", where the reef main current is modified by the overall shape of the coral colony and its neighboring structures, AL was probably located within the "inner benthic boundary layer", defined as the zone where water motion is reduced due to the coral height and internal structure. The existence of these two layers would have reduced intra-colony mixing. Inside each layer and looking even closer, both sampling points could have been within their own momentum boundary layer (a few centimeters thick, and note that we sampled 0.5 cm from the branches) that controls water movement in the close proximity to the coral surface. These thin local layers would have allowed measurable gradients of chemicals, microbes, and genes.

Conclusions

In comparison with the tropical oceans, the two Mo'orean back reef waters sampled showed elevated VOC concentrations only for CS_2, CH_3I, and particularly $CHBr_3$ and CH_2Br_2. Two of the dominant corals, *A. pulchra* and *Pocillopora* sp., were producers and releasers of DMSP, and the former accompanied DMSP with large production of its catabolites DMS, acrylate, and DMSO. However, these compounds were rapidly diluted and consumed in the reef (Xue et al., 2022). The two corals were not remarkable sources of VOC other than DMS. The abundant seaweed *T. ornata* also released DMSP and was directly or indirectly responsible for producing COS and poly-halomethanes, particularly $CHBr_3$ and CH_2Br_2.

Around a colony of *A. pulchra*, large diurnal increases in the concentrations of DMSP, DMS, acrylate, and DMSO closest to the polyps support the hypothesis that these compounds derive from sunlight-induced oxidative stress. rDNA metabarcoding and metagenome analyses of seawater samples around the

colony suggest that DMSP occurrence and its transformation into DMS, acrylate, and DMSO resulted mainly from coral symbionts and their shedding. Large differences in the chemical and microbial compositions next to the living branches and the deeper skeleton colonized by a turf alga, only 10 cm apart, illustrate the hydrodynamic complexity of branched coral colonies, where the coral structure affects the water flow and mixing.

Tropical coral reefs are threatened worldwide as a result of increased stress from global warming, clearer skies, ocean acidification, human uses, and nutrient and pollution dumping (Harborne et al., 2017). Protection and conservation strategies require the development of early reef health/damage indicators as well as a better knowledge of how these complex and ancient ecosystems have evolved fitness and resilience. Volatile and organosulfur compounds have been suggested to be both health indicators and shields against stress, and our work provides new insights into how they operate.

Data availability statement

The datasets presented in this study can be found in online repositories. DMSPC and VOC concentrations can be found at https://zenodo.org/badge/DOI/10.5281/zenodo.7043105.svg. Raw sequences are available at the European Nucleotide Archive (http://www.ebi.ac.uk/ena) under project numbers PRJEB54595 (16S rDNA metabarcoding), PRJEB54596 (18S rDNA metabarcoding) and PRJEB54597 (metagenomics).

Author contributions

MM-N and RS designed the study. MM-N and SG conducted the sample collection and filtration. MM-N, RS, LX, and DK performed the VOC, DMSP, DMSO, and acrylate analyses. MC-B determined microbial abundances by flow cytometry. MM-N isolated DNA and RNA for sequencing. J-FM and JG analyzed the sequencing data for microbial diversity and functional genes. RS, MM-N, J-FM, and JG wrote the manuscript with contributions from all co-authors. All authors contributed to the article and approved the submitted version.

Funding

This project has received funding from the European Research Council (ERC) under the European Union's Horizon 2020 research and innovation program (grant agreement #834162, SUMMIT Advanced Grant to RS). It was also funded by the Spanish Ministry of Science and Innovation (MCIN/AEI, doi: 10.13039/501100011033) through the BIOGAPS grant (CTM2016-81008-R) to RS, the TRAITS grant (PID2019-110011RB-C32) to JMG, the "Severo Ochoa Centre of Excellence" accreditation (CEX2019-000298-S) to the ICM, and predoctoral grants to MM-N (BES-2017-080048) and MC-B (FPU16-01925). LX and DK were supported by funding from the National Science Foundation Chemical Oceanography program (CO-1756907) to DK. SG was supported by an Australian Government Endeavour Research Fellowship.

Acknowledgments

We thank the UC Berkeley Richard Gump Research station staff for logistical support during the field study. Thanks are also extended to Cèlia Marrasé and Pablo Rodríguez-Ros for assistance during the fieldwork, and Yaiza M. Castillo for flow cytometry re-analyses. Computing analyses from both amplicon and metagenomic sequencing data were run at the Marine Bioinformatics Service of the ICM-CSC (http://marbits.icm.csic.es).

Conflict of interest

The authors declare that the research was conducted in the absence of any commercial or financial relationships that could be construed as a potential conflict of interest.

Publisher's note

Supplementary material

The Supplementary Material for this article can be found online at: https://www.frontiersin.org/articles/10.3389/fmars.2022.944141/full#supplementary-material

References

Abrahamsson, K., Choo, K.-S., Pedersеin, M., Johansson, G., and Snoeijs, P. (2003). Effects of temperature on the production of hydrogen peroxide and volatile halocarbons by brackish-water algae. *Phytochemistry* 64, 725–734. doi: 10.1016/S0031-9422(03)00419-9

Alcolombri, U., Ben-Dor, S., Feldmesser, E., Levin, Y., Tawfik, D. S., and Vardi, A. (2015). Identification of the algal dimethyl sulfide–releasing enzyme: A missing link in the marine sulfur cycle. *Science* 348, 1466–1469. doi: 10.1126/science.aab1586

Anders, S., Pyl, P. T., and Huber, W. (2015). HTSeq–a Python framework to work with high- throughput sequencing data. *Bioinformatics* 31, 166–169. doi: 10.1093/bioinformatics/btu638

Apprill, A., Weber, L. G., and Santoro, A. E. (2016). Distinguishing between microbial habitats unravels ecological complexity in coral microbiomes. *mSystems* 1, e00143-16. doi: 10.1128/mSystems.00143-16

Balzano, S., Abs, E., and Leterme, S. (2015). Protist diversity along a salinity gradient in a coastal lagoon. *Aquat. Microb. Ecol.* 74, 263–277. doi: 10.3354/ame01740

Barbera, P., Kozlov, A. M., Czech, L., Morel, B., Darriba, D., Flouri, T., et al. (2019). EPA-Ng: Massively parallel evolutionary placement of genetic sequences. *Systematic Biol.* 68, 365–369. doi: 10.1093/sysbio/syy054

Berger, S. A., and Stamatakis, A. (2011). Aligning short reads to reference alignments and trees. *Bioinformatics* 27, 2068–2075. doi: 10.1093/bioinformatics/btr320

Blezinger, S., Wilhelm, C., and Kesselmeier, J. (2000). Enzymatic consumption of carbonyl sulfide (COS) by marine algae. *Biogeochemistry* 48, 185–197. doi: 10.1023/A:1006134213995

Bolger, A. M., Lohse, M., and Usadel, B. (2014). Trimmomatic: a flexible trimmer for illumina sequence data. *Bioinformatics* 30, 2114–2120. doi: 10.1093/bioinformatics/btu170

Bourne, D. G., Morrow, K. M., and Webster, N. S. (2016). Insights into the coral microbiome: underpinning the health and resilience of reef ecosystems. *Ann. Rev. Microbiol.* 70, 317–340. doi: 10.1146/annurev-micro-102215-095440

Broadbent, A., and Jones, G. (2006). Seasonal and diurnal cycles of dimethylsulfide, dimethylsulfoniopropionate and dimethylsulfoxide at one tree reef lagoon. *Environ. Chem.* 3, 260. doi: 10.1071/EN06011

Broadbent, A. D., Jones, G. B., and Jones, R. J. (2002). DMSP in corals and benthic algae from the great barrier reef. *Est. Coast. Shelf Sci.* 55, 547–555. doi: 10.1006/ecss.2002.1021

Burdett, H. L., Donohue, P. J. C., Hatton, A. D., Alwany, M. A., and Kamenos, N. A. (2013). Spatiotemporal variability of dimethylsulphoniopropionate on a fringing coral reef: The role of reefal carbonate chemistry and environmental variability. *PloS One* 8 (5), e64651. doi: 10.1371/journal.pone.0064651

Callahan, B. J., McMurdie, P. J., Rosen, M. J., Han, A. W., Johnson, A. J. A., and Holmes, S. P. (2016). DADA2: High-resolution sample inference from illumina amplicon data. *Nat. Methods* 13, 581–583. doi: 10.1038/nmeth.3869

Carpenter, L. J., Archer, S. D., and Beale, R. (2012). Ocean-atmosphere trace gas exchange. *Chem. Soc Rev.* 41, 6473–6506. doi: 10.1039/c2cs35121h

Charlson, R. J., Lovelock, J. E., Andreae, M. O., and Warren, S. G. (1987). Oceanic phytoplankton, atmospheric sulfur, cloud albedo and climate. *Nature* 326, 655–661. doi: 10.1038/326655a0

Chaumeil, P.-A., Mussig, A. J., Hugenholtz, P., and Parks, D. H. (2020). GTDB-tk: a toolkit to classify genomes with the genome taxonomy database. *Bioinformatics* 36, 1925–1927. doi: 10.1093/bioinformatics/btz848

Cheng, X., Peterkin, E., and Narangajavana, K. (2007). Wastewater analysis for volatile organic sulfides using purge-and-trap with gas chromatography/mass spectrometry. *Water Environ. Res.* 79, 442–446. doi: 10.2175/106143006X111871

Collado-Mercado, E., Radway, J., and Collier, J. (2010). Novel uncultivated labyrinthulomycetes revealed by 18S rDNA sequences from seawater and sediment samples. *Aquat. Microb. Ecol.* 58, 215–228. doi: 10.3354/ame01361

Curran, A., and Barnard, S. (2021). What is the role of zooxanthellae during coral bleaching? review of zooxanthellae and their response to environmental stress. *S. Afr. J. Sci.* 117, 8639. doi: 10.17159/sajs.2021/8369

Curson, A. R. J., Liu, J., Bermejo Martiínez, A., Green, R. T., Chan, Y., Carrioín, O., et al. (2017). Dimethylsulfoniopropionate biosynthesis in marine bacteria and identification of the key gene in this process. *Nat. Microbiol.* 2, 17009. doi: 10.1038/nmicrobiol.2017.9

Cutter, G. A., Cutter, L. S., and Filippino, K. C. (2004). Sources and cycling of carbonyl sulfide in the Sargasso Sea. *Limnol. Oceanogr.* 49, 555–565. doi: 10.4319/lo.2004.49.2.0555

Czech, L., Barbera, P., and Stamatakis, A. (2020). Genesis and gappa: processing, analyzing and visualizing phylogenetic (placement) data. *Bioinformatics* 36, 3263–3265. doi: 10.1093/bioinformatics/btaa070

Dani, K. G. S., and Loreto, F. (2017). Trade-off between dimethyl sulfide and isoprene emissions from marine phytoplankton. *Trends Plant Sci.* 22, 361–372. doi: 10.1016/j.tplants.2017.01.006

Dawson, R. A., Crombie, A. T., Pichon, P., Steinke, M., McGenity, T. J., and Murrell, J. C. (2021). The microbiology of isoprene cycling in aquatic ecosystems. *Aquat. Microb. Ecol.* 87, 79–98. doi: 10.3354/ame01972

Deschaseaux, E. S. M., Beltran, V. H., Jones, G. B., Deseo, M. A., Swan, H. B., Harrison, P. L., et al. (2014a). Comparative response of DMS and DMSP concentrations in *Symbiodinium* clades C1 and D1 under thermal stress. *J. Exp. Mar. Biol. Ecol.* 459, 181–189. doi: 10.1016/j.jembe.2014.05.018

Deschaseaux, E. S. M., Jones, G. B., Deseo, M. A., Shepherd, K. M., Kiene, R. P., Swan, H. B., et al. (2014b). Effects of environmental factors on dimethylated sulfur compounds and their potential role in the antioxidant system of the coral holobiont. *Limnol. Oceanogr.* 59, 758–768. doi: 10.4319/lo.2014.59.3.0758

Donovan, M. K., Adam, T. C., Shantz, A. A., Speare, K. E., Munsterman, K. S., Rice, M. M., et al. (2020). Nitrogen pollution interacts with heat stress to increase coral bleaching across the seascape. *Proc. Natl. Acad. Sci. U.S.A.* 117, 5351–5357. doi: 10.1073/pnas.1915395117

Eddy, S. R. (2008). A probabilistic model of local sequence alignment that simplifies statistical significance estimation. *PloS Comput. Biol.* 4, e1000069. doi: 10.1371/journal.pcbi.1000069

Elliott, S., Lu, E., and Rowland, F. S. (1987). Carbonyl sulfide hydrolysis as a source of hydrogen sulfide in open ocean seawater. *Geophys. Res. Lett.* 14, 131–134. doi: 10.1029/GL014i002p00131

Exton, D. A., McGenity, T. J., Steinke, M., Smith, D. J., and Suggett, D. J. (2015). Uncovering the volatile nature of tropical coastal marine ecosystems in a changing world. *Glob. Change Biol.* 21, 1383–1394. doi: 10.1111/gcb.12764

Exton, D. A., Suggett, D. J., McGenity, T. J., and Steinke, M. (2013). Chlorophyll-normalized isoprene production in laboratory cultures of marine microalgae and implications for global models. *Limnol. Oceanogr.* 58, 1301–1311. doi: 10.4319/lo.2013.58.4.1301

Fuhrman, J. A., Cram, J. A., and Needham, D. M. (2015). Marine microbial community dynamics and their ecological interpretation. *Nat. Rev. Microbiol.* 13, 133–146. doi: 10.1038/nrmicro3417

Fujise, L., Yamashita, H., Suzuki, G., Sasaki, K., Liao, L. M., and Koike, K. (2014). Moderate thermal stress causes active and immediate expulsion of photosynthetically damaged zooxanthellae (*Symbiodinium*) from corals. *PloS One* 9 (12), e114321. doi: 10.1371/journal.pone.0114321

Galí, M., Ruiz-González, C., Lefort, T., Gasol, J. M., Cardelús, C., Romera-Castillo, C., et al. (2013). Spectral irradiance dependence of sunlight effects on plankton dimethylsulfide production. *Limnol. Oceanogr.* 58, 489–504. doi: 10.4319/lo.2013.58.2.0489

Gardner, S. G., Nielsen, D. A., Laczka, O., Shimmon, R., Beltran, V. H., Ralph, P. J., et al. (2016). Dimethylsulfoniopropionate, superoxide dismutase and glutathione as stress response indicators in three corals under short-term hyposalinity stress. *Proc. R. Soc B.* 283, 20152418. doi: 10.1098/rspb.2015.2418

Garren, M., Son, K., Raina, J.-B., Rusconi, R., Menolascina, F., Shapiro, O. H., et al. (2014). A bacterial pathogen uses dimethylsulfoniopropionate as a cue to target heat-stressed corals. *ISME J.* 8, 999–1007. doi: 10.1038/ismej.2013.210

Gong, J., Shi, F., Ma, B., Dong, J., Pachiadaki, M., Zhang, X., et al. (2015). Depth shapes α- and β-diversities of microbial eukaryotes in surficial sediments of coastal ecosystems: Diversity and biogeography of benthic microeukaryotes. *Environ. Microbiol.* 17, 3722–3737. doi: 10.1111/1462-2920.12763

Goodwin, K. D., North, W. J., and Lidstrom, M. E. (1997). Production of bromoform and dibromomethane by giant kelp: Factors affecting release and comparison to anthropogenic bromine sources. *Limnol. Oceanogr.* 42, 1725–1734. doi: 10.4319/lo.1997.42.8.1725

Guibert, I., Bourdreux, F., Bonnard, I., Pochon, X., Dubousquet, V., Raharivelomanana, P., et al. (2020). Dimethylsulfoniopropionate concentration in coral reef invertebrates varies according to species assemblages. *Sci. Rep.* 10, 9922. doi: 10.1038/s41598-020-66290-5

Guillou, L., Bachar, D., Audic, S., Bass, D., Berney, C., Bittner, L., et al. (2012). The protist ribosomal reference database (PR2): a catalog of unicellular eukaryote small sub-unit rRNA sequences with curated taxonomy. *Nucleic Acids Res.* 41, D597–D604. doi: 10.1093/nar/gks1160

Harborne, A. R., Rogers, A., Bozec, Y.-M., and Mumby, P. J. (2017). Multiple stressors and the functioning of coral reefs. *Annu. Rev. Mar. Sci.* 9, 445–468. doi: 10.1146/annurev-marine-010816-060551

Haydon, T. D., Seymour, J. R., and Suggett, D. J. (2018). Soft corals are significant DMSP producers in tropical and temperate reefs. *Mar. Biol.* 165, 109. doi: 10.1007/s00227-018-3367-2

Hemond, E. M., and Vollmer, S. V. (2015). Diurnal and nocturnal transcriptomic variation in the Caribbean staghorn coral, *Acropora cervicornis*. *Mol. Ecol.* 24, 4460–4473. doi: 10.1111/mec.13320

Hill, R. W., Dacey, W. H., and Krupp, D. A. (1995). Dimethylsulfoniopropionate in reef corals. *Bull. Mar. Sci.* 57, 489–494.

Hoegh-Guldberg, O., McCloskey, L. R., and Muscatine, L. (1987). Expulsion of zooxanthellae by symbiotic cnidarians from the red Sea. *Coral Reefs* 5, 201–204. doi: 10.1007/BF00300964

Hoegh-Guldberg, O., Poloczanska, E. S., Skirving, W., and Dove, S. (2017). Coral reef ecosystems under climate change and ocean acidification. *Front. Mar. Sci.* 29 doi: 10.3389/fmars.2017.00158

Hopkins, F. E., Bell, T. G., Yang, M., Suggett, D. J., and Steinke, M. (2016). Air exposure of coral is a significant source of dimethylsulfide (DMS) to the atmosphere. *Sci. Rep.* 6, 36031. doi: 10.1038/srep36031

Howard, E. C., Henriksen, J. R., Buchan, A., Reisch, C. R., Bürgmann, H., Welsh, R., et al. (2006). Bacterial taxa that limit sulfur flux from the ocean. *Science* 314, 649–652. doi: 10.1126/science.1130657

Hyatt, D., Chen, G.-L., LoCascio, P. F., Land, M. L., Larimer, F. W., and Hauser, L. J. (2010). Prodigal: prokaryotic gene recognition and translation initiation site identification. *BMC Bioinf.* 11, 119. doi: 10.1186/1471-2105-11-119

Jackson, R. L., Gabric, A. J., and Cropp, R. (2020). Coral reefs as a source of climate-active aerosols. *PeerJ.* 8, e10023. doi: 10.7717/peerj.10023

Jones, G. B. (2015). "The reef sulfur cycle: Influence on climate and ecosystem services," in *Ethnobiology of corals and coral reefs*. Eds. N. E. Narchi and L. L. Price (Switzerland: Springer International Publishing), 27–57. doi: 10.1007/978-3-319-23763-3_3

Kettle, A. J., Rhee, T. S., von Hobe, M., Poulton, A., Aiken, J., and Andreae, M. O. (2001). Assessing the flux of different volatile sulfur gases from the ocean to the atmosphere. *J. Geophys. Res.* 106, 12193–12209. doi: 10.1029/2000JD900630

Kiene, R. P., and Slezak, D. (2006). Low dissolved DMSP concentrations in seawater revealed by small-volume gravity filtration and dialysis sampling: Filtration and dialysis for dissolved DMSP. *Limnol. Oceanogr. Methods* 4, 80–95. doi: 10.4319/lom.2006.4.80

Kim, K. H., and Andreae, M. O. (1992). Carbon disulfide in the estuarine, coastal and oceanic environments. *Mar. Chem.* 40, 179–1971992. doi: 10.1016/0304-4203(92)90022-3

Kinsey, J. D., and Kieber, D. J. (2016). Microwave preservation method for DMSP, DMSO, and acrylate in unfiltered seawater and phytoplankton culture samples: Microwave sample preservation method. *Limnol. Oceanogr. Methods* 14, 196–209. doi: 10.1002/lom3.10081

Kinsey, J. D., Kieber, D. J., and Neale, P. J. (2016). Effects of iron limitation and UV radiation on *Phaeocystis antarctica* growth and dimethylsulfoniopropionate, dimethylsulfoxide and acrylate concentrations. *Environ. Chem.* 13, 195. doi: 10.1071/EN14275

Klemetsen, T., Raknes, I. A., Fu, J., Agafonov, A., Balasundaram, S. V., Tartari, G., et al. (2018). The MAR databases: development and implementation of databases specific for marine metagenomics. *Nucleic Acids Res.* 46, D692–D699. doi: 10.1093/nar/gkx1036

Koid, A., Nelson, W. C., Mraz, A., and Heidelberg, K. B. (2012). Comparative analysis of eukaryotic marine microbial assemblages from 18S rRNA gene and gene transcript clone libraries by using different methods of extraction. *Appl. Environ. Microbiol.* 78, 3958–3965. doi: 10.1128/AEM.06941-11

Kuek, F. W. I., Motti, C. A., Zhang, J., Cooke, I. R., Todd, J. D., Miller, D. J., et al. (2022). DMSP production by coral-associated bacteria. *Front. Mar. Sci* 9. doi: 10.3389/fmars.2022.869574

Kutti, T., Johnsen, I. A., Skaar, K. S., Ray, J. L., Husa, V., and Dahlgren, T. G. (2020). Quantification of eDNA to map the distribution of cold-water coral reefs. *Front. Mar. Sci.* 7. doi: 10.3389/fmars.2020.00446

Lana, A., Bell, T. G., Simoí, R., Vallina, S. M., Ballabrera-Poy, J., Kettle, A. J., et al. (2011). An updated climatology of surface dimethlysulfide concentrations and emission fluxes in the global ocean. *Global Biogeochem. Cycles* 25, GB1004. doi: 10.1029/2010GB003850

Landa, M., Burns, A. S., Durham, B. P., Esson, K., Nowinski, B., Sharma, S., et al. (2019). Sulfur metabolites that facilitate oceanic phytoplankton–bacteria carbon flux. *ISME J.* 13, 2536–2550. doi: 10.1038/s41396-019-0455-3

Langmead, B., and Salzberg, S. L. (2012). Fast gapped-read alignment with bowtie 2. *Nat. Methods* 9, 357–359. doi: 10.1038/nmeth.1923

Lawson, C. A., Raina, J.-B., Deschaseaux, E., Hrebien, V., Possell, M., Seymour, J. R., et al. (2021). Heat stress decreases the diversity, abundance and functional potential of coral gas emissions. *Global Change Biol.* 27, 879–891. doi: 10.1111/gcb.15446

Lawson, C. A., Seymour, J. R., Possell, M., Suggett, D. J., and Raina, J.-B. (2020). The volatilomes of symbiodiniaceae-associated bacteria are influenced by chemicals derived from their algal partner. *Front. Mar. Sci.* 7. doi: 10.3389/fmars.2020.00106

Leedham, E. C., Hughes, C., Keng, F. S. L., Phang, S.-M., Malin, G., and Sturges, W. T. (2013). Emission of atmospherically significant halocarbons by naturally occurring and farmed tropical macroalgae. *Biogeosciences* 10, 3615–3633. doi: 10.5194/bg-10-3615-2013

Lennartz, S. T., Marandino, C. A., von Hobe, M., Andreae, M. O., Aranami, K., Atlas, E., et al. (2020). Marine carbonyl sulfide (OCS) and carbon disulfide (CS_2): a compilation of measurements in seawater and the marine boundary layer. *Earth Syst. Sci. Data* 12, 591–609. doi: 10.5194/essd-12-591-2020

Letunic, I., and Bork, P. (2021). Interactive tree of life (iTOL) v5: an online tool for phylogenetic tree display and annotation. *Nucleic Acids Res.* 49, W293–W296. doi: 10.1093/nar/gkab301

Li, W., and Godzik, A. (2006). Cd-hit: a fast program for clustering and comparing large sets of protein or nucleotide sequences. *Bioinformatics* 22, 1658–1659. doi: 10.1093/bioinformatics/btl158

Li, H., Handsaker, B., Wysoker, A., Fennell, T., Ruan, J., Homer, N., et al. (2009). The sequence alignment/map format and SAMtools. *Bioinformatics* 25, 2078–2079. doi: 10.1093/bioinformatics/btp352

Li, D., Luo, R., Liu, C.-M., Leung, C.-M., Ting, H.-F., Sadakane, K., et al. (2016). MEGAHIT v1.0: A fast and scalable metagenome assembler driven by advanced methodologies and community practices. *Methods* 102, 3–11. doi: 10.1016/j.ymeth.2016.02.020

Lim, Y.-K., Phang, S.-M., Abdul Rahman, N., Sturges, W. T., and Malin, G. (2017). Halocarbon emissions from marine phytoplankton and climate change. *Int. J. Environ. Sci. Technol.* 14, 1355–1370. doi: 10.1007/s13762-016-1219-5

Maire, J., Girvan, S. K., Barkla, S. E., Perez-Gonzalez, A., Suggett, D. J., Blackall, L. L., et al. (2021). Intracellular bacteria are common and taxonomically diverse in cultured and in hospite algal endosymbionts of coral reefs. *ISME J.* 15, 2028–2042. doi: 10.1038/s41396-021-00902-4

Martin, M. (2011). Cutadapt removes adapter sequences from high-throughput sequencing reads. *EMBnet J.* 17, 10. doi: 10.14806/ej.17.1.200

Massana, R., Murray, A. E., Preston, C. M., and DeLong, E. F. (1997). Vertical distribution and phylogenetic characterization of marine planktonic archaea in the Santa Barbara channel. *Appl. Environ. Microbiol.* 63, 50–56. doi: 10.1128/aem.63.1.50-56.1997

McGenity, T. J., Crombie, A. T., and Murrell, J. C. (2018). Microbial cycling of isoprene, the most abundantly produced biological volatile organic compound on earth. *ISME J.* 12, 931–941. doi: 10.1038/s41396-018-0072-6

Meskhidze, N., Sabolis, A., Reed, R., and Kamykowski, D. (2015). Quantifying environmental stress-induced emissions of algal isoprene and monoterpenes using laboratory measurements. *Biogeosciences* 12, 637–651. doi: 10.5194/bg-12-637-2015

Moore, R. M., Webb, M., Tokarczyk, R., and Wever, R. (1996). Bromoperoxidase and iodoperoxidase enzymes and production of halogenated methanes in marine diatom cultures. *J. Geophys. Res.* 101, 20899–20908. doi: 10.1029/96JC01248

Nguyen, L.-T., Schmidt, H. A., von Haeseler, A., and Minh, B. Q. (2015). IQ-TREE: A fast and effective stochastic algorithm for estimating maximum-likelihood phylogenies. *Mol. Biol. Evol.* 32, 268–274. doi: 10.1093/molbev/msu300

Nishimura, Y., and Yoshizawa, S. (2022). The OceanDNA MAG catalog contains over 50,000 prokaryotic genomes originated from various marine environments. *Sci Data* 9, 305. doi: 10.1038/s41597-022-01392-5

Nitschke, M. R., Gardner, S. G., Goyen, S., Fujise, L., Camp, E. F., Ralph, P. J., et al. (2018). Utility of photochemical traits as diagnostics of thermal tolerance amongst great barrier reef corals. *Front. Mar. Sci.* 5 (45). doi: 10.3389/fmars.2018.00045

Ohsawa, N., Ogata, Y., Okada, N., and Itoh, N. (2001). Physiological function of bromoperoxidase in the red marine alga, *Corallina pilulifera*: production of bromoform as an allelochemical and the simultaneous elimination of hydrogen peroxide. *Phytochemistry* 58, 683–692. doi: 10.1016/S0031-9422(01)00259-X

Oksanen, J., Blanchet, F. G., Friendly, M., Kindt, R., Legendre, P., McGlinn, D., et al. (2021) *Vegan: Community ecology package*. Available at: https://CRAN.R-project.org/package=vegan.

Ooki, A., Nomura, D., Nishino, S., Kikuchi, T., and Yokouchi, Y. (2015). A global-scale map of isoprene and volatile organic iodine in surface seawater of the Arctic, Northwest pacific, Indian, and southern oceans. *J. Geophys. Res. Ocean.* 120, 4108–4128. doi: 10.1002/2014JC010519

Paoli, L., Ruscheweyh, H.-J., Forneris, C. C., Kautsar, S., Clayssen, Q., Salazar, G., et al. (2022). Uncharted biosynthetic potential of the ocean microbiome. *Nature* 607, 111–118 doi: 10.1038/s41586-022-04862-3

Parada, A. E., Needham, D. M., and Fuhrman, J. A. (2016). Every base matters: assessing small subunit rRNA primers for marine microbiomes with mock communities, time series and global field samples: Primers for marine microbiome studies. *Environ. Microbiol.* 18, 1403–1414. doi: 10.1111/1462-2920.13023

Pruesse, E., Quast, C., Knittel, K., Fuchs, B. M., Ludwig, W., Peplies, J., et al. (2007). SILVA: a comprehensive online resource for quality checked and aligned ribosomal RNA sequence data compatible with ARB. *Nucleic Acids Res.* 35, 7188–7196. doi: 10.1093/nar/gkm864

Raina, J.-B., Dinsdale, E. A., Willis, B. L., and Bourne, D. G. (2010). Do the organic sulfur compounds DMSP and DMS drive coral microbial associations? *Trends Microbiol.* 18, 101–108. doi: 10.1016/j.tim.2009.12.002

Raina, J.-B., Tapiolas, D. M., Foreêt, S., Lutz, A., Abrego, D., Ceh, J., et al. (2013). DMSP biosynthesis by an animal and its role in coral thermal stress response. *Nature* 502, 677–680. doi: 10.1038/nature12677

Raina, J.-B., Tapiolas, D., Willis, B. L., and Bourne, D. G. (2009). Coral-associated bacteria and their role in the biogeochemical cycling of sulfur. *Appl. Environ. Microbiol.* 75, 3492–3501. doi: 10.1128/AEM.02567-08

R Development Core Team (2021) *R: A language and environment for statistical computing*. Available at: http://www.r-project.org/.

Richter, U., and Wallace, D. W. R. (2004). Production of methyl iodide in the tropical Atlantic ocean. *Geophys. Res. Lett.* 31, L23S03. doi: 10.1029/2004GL020779

Rohwer, F., Segritan, V., Azam, F., and Knowlton, N. (2002). Diversity and distribution of coral-associated bacteria. *Mar. Ecol. Prog. Ser.* 243, 1–10. doi: 10.3354/meps243001

Saiz-López, A., and von Glasow, R. (2012). Reactive halogen chemistry in the troposphere. *Chem. Soc Rev.* 41, 6448–6472. doi: 10.1039/c2cs35208g

Schneider, K., Levy, O., Dubinsky, Z., and Ereza, J. (2009). *In situ* diel cycles of photosynthesis and calcification in hermatypic corals. *Limnol. Oceanogr.* 54, 1995–2002. doi: 10.4319/lo.2009.54.6.1995

Schrameyer, V., Krämer, W., Hill, R., Jeans, J., Larkum, A., Bischof, K., et al. (2016). Under high light stress two indo-pacific coral species display differential photodamage and photorepair dynamics. *Mar. Biol.* 163, 168. doi: 10.1007/s00227-016-2940-9

Seo, H.-S., Kwon, K. K., Yang, S.-H., Lee, H.-S., Bae, S. S., Lee, J.-H., et al. (2009). *Marinoscillum* gen. nov., a member of the family "Flexibacteraceae", with marinoscillum pacificum sp. nov. from a marine sponge and *Marinoscillum furvescens* nom. rev., comb. nov. *Int. J. Syst. Evol. Microbiol.* 59, 1204–1208. doi: 10.1099/ijs.0.004317-0

Shashar, N., Kinane, S., Jokiel, P. L., and Patterson, M. R. (1996). Hydromechanical boundary layers over a coral reef. *J. Exp. Mar. Biol. Ecol.* 199, 17–28. doi: 10.1016/0022-0981(95)00156-5

Simó, R. (2001). Production of atmospheric sulfur by oceanic plankton: biogeochemical, ecological and evolutionary links. *Trends Ecol. Evol.* 16, 287–294. doi: 10.1016/S0169-5347(01)02152-8

Sunda, W., Kieber, D. J., Kiene, R. P., and Huntsman, S. (2002). An antioxidant function for DMSP and DMS in marine algae. *Nature* 418, 317–320. doi: 10.1038/nature00851

Swan, H. B., Crough, R. W., Vaattovaara, P., Jones, G. B., Deschaseaux, E. S. M., Eyre, B. D., et al. (2016). Dimethyl sulfide and other biogenic volatile organic compound emissions from branching coral and reef seawater: potential sources of secondary aerosol over the great barrier reef. *J. Atmos. Chem.* 73, 303–328. doi: 10.1007/s10874-016-9327-7

Swan, H. B., Deschaseaux, E. S. M., Jones, G. B., and Eyre, B. D. (2017). Quantification of dimethylsulfoniopropionate (DMSP) in *Acropora* spp. of reef-building coral using mass spectrometry with deuterated internal standard. *Anal. Bioanal. Chem.* 409, 1929–1942. doi: 10.1007/s00216-016-0141-5

Tandon, K., Lu, C. Y., Chiang, P. W., Wada, N., Yang, S.-H-, Chan, Y.-H., et al. (2020). Comparative genomics: Dominant coral-bacterium *Endozoicomonas acroporae* metabolizes dimethylsulfoniopropionate (DMSP). *ISME J.* 14, 1290–1303. doi: 10.1038/s41396-020-0610-x

Tapiolas, D. M., Motti, C. A., Holloway, P., and Boyle, S. G. (2010). High levels of acrylate in the great barrier reef coral *Acropora millepora*. *Coral Reefs* 29, 621–625. doi: 10.1007/s00338-010-0608-3

Todd, J. D., Curson, A. R. J., Sullivan, M. J., Kirkwood, M., and Johnston, A. W. B. (2012a). The *Ruegeria pomeroyi* acuI gene has a role in DMSP catabolism and resembles yhdH of e. coli and other bacteria in conferring resistance to acrylate. *PloS One* 7 (4), e35947. doi: 10.1371/journal.pone.0035947

Tyssebotn, I. M. B., Kinsey, J. D., Kieber, D. J., Kiene, R. P., Rellinger, A. N., and Motard-Coêteí, J. (2017). Concentrations, biological uptake, and respiration of dissolved acrylate and dimethylsulfoxide in the northern gulf of Mexico. *Limnol. Oceanogr.* 62, 1198–1218. doi: 10.1002/lno.10495

Vd'ačnyí, P., Bourland, W. A., Orsi, W., Epstein, S. S., and Foissner, W. (2011). Phylogeny and classification of the litostomatea (Protista, ciliophora), with emphasis on free-living taxa and the 18S rRNA gene. *Mol. Phylogenet. Evol.* 59, 510–522. doi: 10.1016/j.ympev.2011.02.016

Wang, Q., Garrity, G. M., Tiedje, J. M., and Cole, J. R. (2007). Naiüve Bayesian classifier for rapid assignment of rRNA sequences into the new bacterial taxonomy. *Appl. Environ. Microbiol.* 73, 5261–5267. doi: 10.1128/AEM.00062-07

Washburn, L., and Brooks, A. (2022). "Gump station meteorological data". In: *Environmental data initiative*. MCR LTER: Coral Reef. knb-lter-mcr.9.46 doi: 10.6073/pasta/6d30349193252011bed853ae421d8b0d

Weber, L., Gonzalez-Díaz, P., Armenteros, M., and Apprill, A. (2019). The coral ecosphere: a unique coral reef habitat that fosters coral–microbial interactions. *Limnol. Oceanogr.* 64, 2373–2388. doi: 10.1002/lno.11190

Weis, V. M. (2008). Cellular mechanisms of cnidarian bleaching: stress causes the collapse of symbiosis. *J. Exp. Biol.* 211, 3059–3066. doi: 10.1242/jeb.009597

Woodhead, A. J., Hicks, C. C., Norström, A. V., Williams, G. J., and Graham, N. A. J. (2019). Coral reef ecosystem services in the anthropocene. *Funct. Ecol.* 33, 1023–1034. doi: 10.1111/1365-2435.13331

Xie, H., Moore, R. M., and Miller, W. L. (1998). Photochemical production of carbon disulphide in seawater. *J. Geophys. Res.* 103, 5635–5644. doi: 10.1029/97JC02885

Xie, H., Scarratt, M. G., and Moore, R. M. (1999). Carbon disulphide production in laboratory cultures of marine phytoplankton. *Atmos. Environ.* 33, 3445–3453. doi: 10.1016/S1352-2310(98)00430-0

Xue, L., Kieber, D. J., Masdeu-Navarro, M., Cabrera-Brufau, M., Rodríguez-Ros, P., Gardner, S. G., et al. (2022). Concentrations and biological consumption of acrylate and DMSP in the tropical pacific and coral reef ecosystem in mo'orea, French Polynesia. *Front. Mar. Sci.* 9, 911522. doi: 10.3389/fmars.2022.911522

Yokouchi, Y., Ooki, A., Hashimoto, S., and Itoh, N. (2014). "A study on the production and emission of marine-derived volatile halocarbons," in *Western Pacific air-Sea interaction study*. Eds. M. Uematsu, Y. Yokouchi, Y. Watanabe, S. Takeda and Y. Yamanaka (Tokyo: TERRAPUB), 1–25. doi: 10.5047/w-pass.a01.001

Yost, D., and Mitchelmore, C. (2009). Dimethylsulfoniopropionate (DMSP) lyase activity in different strains of the symbiotic alga *Symbiodinium microadriaticum*. *Mar. Ecol. Prog. Ser.* 386, 61–70. doi: 10.3354/meps08031

Zhu, F., Massana, R., Not, F., Marie, D., and Vaulot, D. (2005). Mapping of picoeucaryotes in marine ecosystems with quantitative PCR of the 18S rRNA gene. *FEMS Microbiol. Ecol.* 52, 79–92. doi: 10.1016/j.femsec.2004.10.006

Ziska, F., Quack, B., Abrahamsson, K., Archer, S. D., Atlas, E., Bell, T., et al. (2013). Global sea-to- air flux climatology for bromoform, dibromomethane and methyl iodide. *Atmos. Chem. Phys.* 13, 8915–8934. doi: 10.5194/acp-13-8915-2013